Tail-anchored PEX26 targets peroxisomes via a PEX19-dependent and TRC40-independent class I pathway

Yuichi Yagita,[1] Takahide Hiromasa,[1] and Yukio Fujiki[1,2]

[1]Graduate School of Systems Life Sciences and [2]Department of Biology, Faculty of Sciences, Kyushu University, Higashi-ku, Fukuoka 812-8581, Japan

Tail-anchored (TA) proteins are anchored into cellular membranes by a single transmembrane domain (TMD) close to the C terminus. Although the targeting of TA proteins to peroxisomes is dependent on PEX19, the mechanistic details of PEX19-dependent targeting and the signal that directs TA proteins to peroxisomes have remained elusive, particularly in mammals. The present study shows that PEX19 formed a complex with the peroxisomal TA protein PEX26 in the cytosol and translocated it directly to peroxisomes by interacting with the peroxisomal membrane protein PEX3. Unlike in yeast, the adenosine triphosphatase TRC40, which delivers TA proteins to the endoplasmic reticulum, was dispensable for the peroxisomal targeting of PEX26. Moreover, the basic amino acids within the luminal domain of PEX26 were essential for binding to PEX19 and thereby for peroxisomal targeting. Finally, our results suggest that a TMD that escapes capture by TRC40 and is followed by a highly basic luminal domain directs TA proteins to peroxisomes via the PEX19-dependent route.

Introduction

Tail-anchored (TA) proteins are anchored into the lipid bilayer by a single transmembrane domain (TMD) close to the C terminus and display their N-terminal domain to the cytosol (Kutay et al., 1993). These TA proteins are found in virtually all cellular membranes and play essential roles in various processes that range from protein translocation to vesicular trafficking, apoptosis, and many others. Therefore, their correct targeting and localization are of basic cellular importance across all eukaryotes (Borgese et al., 2007). Recent studies have increased our knowledge of the machineries and mechanisms by which TA proteins are targeted to and inserted into the ER membrane. Of several proposed pathways, the GET pathway that involves a cytosolic ATPase (mammalian TRC40 or yeast Get3) is now widely accepted as the dominant targeting pathway (Borgese and Fasana, 2011; Hegde and Keenan, 2011).

In contrast, the pathway and molecular mechanism for the delivery of TA proteins to peroxisomes remain elusive, mainly because two pathways are proposed for the import of peroxisomal membrane proteins (PMPs): a "direct import" pathway and an "ER to peroxisome trafficking" pathway, both of which are mediated by PEX3, PEX19, and in mammals, PEX16 (Fujiki et al., 2006; Ma et al., 2011; Nuttall et al., 2011; Rucktäschel et al., 2011). In the former pathway, PMPs are imported directly from the cytosol to peroxisomes. PEX19 functions as a chaperone and soluble receptor for PMPs (Jones et al., 2004; Matsuzono et al., 2006). PEX3 provides a docking site for PEX19, probably PMP-loaded PEX19, at the membrane (Fang et al., 2004). PEX16 acts as a membrane receptor for the soluble PEX3–PEX19 complex during PEX3 import (Matsuzaki and Fujiki, 2008). In contrast, in the latter pathway, PMPs are inserted into the ER and then sorted to peroxisomes. PEX3 and PEX19 mediate the sorting of PMPs from the ER to peroxisomes (Hoepfner et al., 2005; Lam et al., 2010; van der Zand et al., 2010). PEX16 was reported to recruit PEX3 to the ER (Kim et al., 2006).

Earlier studies on two peroxisomal TA proteins, yeast Pex15p and plant peroxisomal ascorbate peroxidase, suggested that they traffic through the ER en route to peroxisomes (Elgersma et al., 1997; Mullen et al., 1999; Schuldiner et al., 2008).

Correspondence to Yukio Fujiki: yfujiki@kyudai.jp

Abbreviations used in this paper: AOx, acyl-CoA oxidase; Cyt b_5, cytochrome b_5; Fis1, fission1; MOM, mitochondrial outer membrane; mPTS, peroxisomal membrane-targeting signal; PMP, peroxisomal membrane protein; PTS1, peroxisomal targeting signal type 1; RRL, rabbit reticulocyte lysate; TA, tail anchored; TMD, transmembrane domain; VAMP2, vesicular-associated protein 2; WT, wild type.

The Rockefeller University Press $30.00
J. Cell Biol. Vol. 200 No. 5 651–666
www.jcb.org/cgi/doi/10.1083/jcb.201211077

Recently, Get3 was shown to interact physically with Pex15p and, together with other components of the GET (guided entry of TA proteins) pathway, to mediate its insertion into the ER (Schuldiner et al., 2008; Jonikas et al., 2009; Costanzo et al., 2010). Moreover, the yeast Pex19p-dependent budding of Pex15p-containing vesicles from the ER was reconstituted in vitro (Lam et al., 2010). In contrast, studies using mammalian PEX26, a TA protein functionally homologous to Pex15p, showed that the import of PEX26 requires PEX19 (Halbach et al., 2006) and that cell-free synthesized PEX26 is transported to isolated peroxisomes in a PEX19-stimulated manner (Matsuzono and Fujiki, 2006), implying PEX19-dependent direct import. Indeed, two PEX19 binding sites, one overlapping with the TMD and the other in the hydrophilic luminal region (hereafter referred to as C segment), were identified in PEX26 as well as Pex15p (Halbach et al., 2006); however, the precise route and molecular mechanisms underlying the import of peroxisomal TA proteins in mammalian cells remain unclear, including the function of PEX19, the requirement of a membrane component, and the involvement of TRC40. Furthermore, the signal that directs TA proteins to mammalian peroxisomes remains to be characterized.

The present study analyzed the import of PEX26 using a semi-intact cell system and showed that PEX19 forms a complex with PEX26 in the cytosol and delivers it to peroxisomes in a manner dependent on the PEX3–PEX19 interaction. Neither the targeting nor the insertion of PEX26 requires ATP, indicating TRC40-independent import. Our results indicate that PEX26 follows the PEX19- and PEX3-mediated direct import pathway. Moreover, the data demonstrate that basic residues within the C segment of TA proteins are important but not sufficient for peroxisomal targeting. Peroxisomal TA proteins seem to require both a relatively hydrophilic TMD and a highly basic C segment to escape capture by TRC40 and ensure binding to PEX19. Based on these and earlier findings, a model for the selective targeting of TA proteins to the appropriate organelle membrane in mammalian cells is suggested.

Results

PEX19 is required for peroxisomal targeting of PEX26

PEX19, a predominantly cytosolic protein, was shown to be involved in the import of the mammalian peroxisomal TA protein PEX26 (Halbach et al., 2006). This result was confirmed by siRNA-mediated knockdown of *PEX19*. Transfection of *PEX19*-specific siRNAs into HeLa cells resulted in a prominent decrease in the level of PEX19, whereas the level of PEX14, a PMP, was not affected (Fig. S1 A). In control siRNA-treated cells, newly synthesized EGFP-fused PEX26 (EGFP-PEX26) was colocalized with proteins harboring peroxisomal targeting signal type 1 (PTS1), indicating the translocation of EGFP-PEX26 to peroxisomes (Fig. S1 B, a–c). In contrast, although the peroxisomal targeting of EGFP-PEX26 was still observed to some extent, EGFP-PEX26 was mistargeted to mitochondria in *PEX19* siRNA-treated cells, as demonstrated by colocalization with cytochrome *c*, a mitochondrial marker protein (Fig. S1 B, d–e). The frequency of cells showing mislocalization of EGFP-PEX26 was >60% in *PEX19* siRNA-treated cells, whereas that in control siRNA-treated cells was ∼30% (Fig. S1 B, graph). Mislocalization observed in control siRNA-treated cells was probably caused by overexpression; overexpression of EGFP-PEX26 readily resulted in its targeting to mitochondria even in untreated cells (unpublished data). These observations are consistent with the previous study (Halbach et al., 2006) and demonstrate that *PEX19* knockdown impairs the peroxisomal import of EGFP-PEX26.

PEX19 forms soluble complexes with PEX26 in the cytosol and maintains it in an import-competent state

As a step toward delineating the precise role of PEX19 in the biogenesis of PEX26, FLAG-tagged PEX26 (FLAG-PEX26) was expressed with or without HA-tagged PEX19 (HA-PEX19) in CHO-K1 cells, and its subcellular distribution was verified by cell fractionation. FLAG-PEX26 was detected exclusively in the organelle fraction when expressed alone, whereas it was found both in the cytosolic and in the organelle fractions when coexpressed with HA-PEX19 (Fig. 1 A, lanes 1–6). The steady-state level of FLAG-PEX26 was significantly higher in HA-PEX19–expressing cells than in mock-transfected cells, implying that FLAG-PEX26 was stabilized, most likely in the cytosol, by HA-PEX19. A further coimmunoprecipitation assay revealed that HA-PEX19 indeed formed a soluble complex with FLAG-PEX26 in the cytosol (Fig. 1 A, lanes 7–9). As suggested in a previous study (Halbach et al., 2006), the interaction of PEX19 with PEX26 is dependent on the peroxisomal membrane-targeting signal (mPTS); HA-PEX19 failed to interact with FLAG-PEX26ΔC, a variant lacking the TMD and the C segment (Fig. S2). These findings are consistent with previous studies suggesting that PEX19 functions as a chaperone and/or soluble receptor for nascent PMPs (Sacksteder et al., 2000; Jones et al., 2004; Rottensteiner et al., 2004; Shibata et al., 2004; Halbach et al., 2005; Matsuzono and Fujiki, 2006).

To examine whether the PEX19–PEX26 complex in the cytosol is an import-competent intermediate, import assays were performed in vitro using semi-intact cells. HeLa cells were treated with digitonin to selectively permeabilize the plasma membrane and subsequently incubated with the cytosolic fraction obtained from CHO-K1 cells coexpressing HA-PEX26 and FLAG-PEX19. Immunofluorescence microscopy analysis showed that HA-PEX26 colocalized with catalase, a peroxisomal matrix protein, indicating that HA-PEX26 was translocated to peroxisomes (Fig. 1 B, a and b). When semi-intact cells were incubated as a control with the cytosolic fraction of CHO-K1 cells expressing HA-PEX26 alone, peroxisomal targeting of HA-PEX26 was not observed (Fig. 1 B, c and d), which is consistent with the fact that PEX26 was recovered exclusively in the organelle fraction when expressed alone (Fig. 1 A). To confirm that PEX26 complexed with PEX19 is translocated to peroxisomes, in vitro import assays were performed using isolated PEX19–PEX26 complexes. FLAG-PEX19–HA-PEX26 complexes formed in the cytosol were immunoaffinity purified with the anti-FLAG antibody conjugated to agarose beads

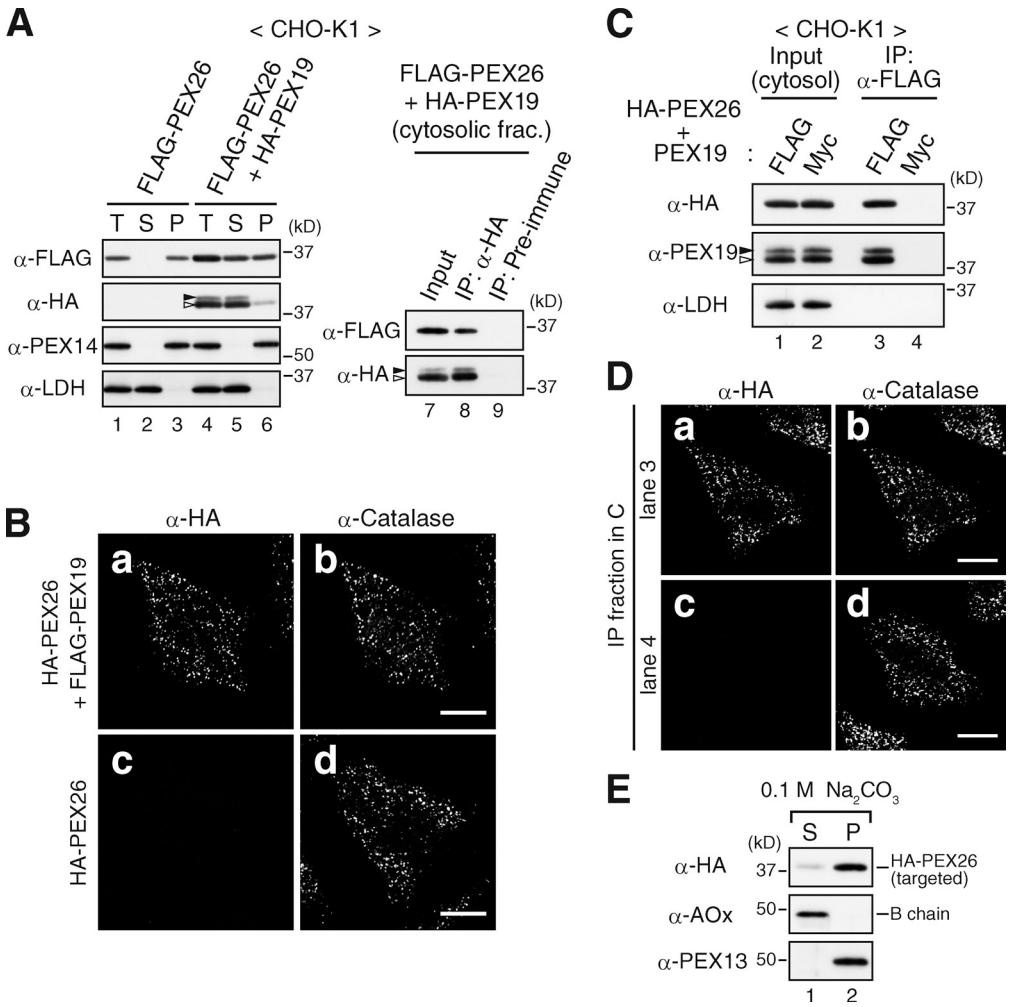

Figure 1. **PEX19 forms a soluble complex with PEX26 in the cytosol and maintains its import-competent state.** (A, left) CHO-K1 cells transiently transfected with *FLAG-PEX26* and either empty vector (lanes 1–3) or *HA-PEX19* (lanes 4–6) were fractionated into postnuclear supernatant (T, total), cytosolic (S, supernatant), and organelle (P, pellet) fractions. Equal aliquots of the respective fractions were analyzed by SDS-PAGE and immunoblotting using the indicated antibodies. Lactate dehydrogenase (LDH) and PEX14, a PMP, are markers for supernatant and pellet fractions, respectively. (right) Supernatant fraction obtained from CHO-K1 cells coexpressing FLAG-PEX26 and HA-PEX19 was subjected to immunoprecipitation with the anti-HA antibody (lane 8) or preimmune serum (lane 9). Immunoprecipitates and input (10%; lane 7) were analyzed by immunoblotting using the indicated antibodies. (B) HeLa cells were semipermeabilized and incubated at 26°C for 1 h with the cytosolic fraction of CHO-K1 cells expressing either HA-PEX26 plus FLAG-PEX19 (a and b) or HA-PEX26 alone (c and d). Cells were immunostained with antibodies against HA and catalase, a peroxisomal matrix protein. (C) Cytosolic fractions of CHO-K1 cells coexpressing HA-PEX26 and either FLAG-PEX19 (lanes 1 and 3) or Myc-PEX19 (lanes 2 and 4) were subjected to immunoprecipitation with anti-FLAG agarose beads. Immunoprecipitates were eluted with FLAG peptides and analyzed by immunoblotting using the indicated antibodies. Input (10%) was loaded in lanes 1 and 2. (D) In vitro import assay was performed as in B using the eluted fraction shown in C (lane 3) containing FLAG-PEX19–HA-PEX26 complexes (a and b). Another eluted fraction shown in C (lane 4) was used as a control (c and d). Cells were immunostained as in B. (E) Cells shown in D (top) were treated with 0.1 M Na_2CO_3 and separated into soluble (supernatant) and membrane (pellet) fractions. Equal aliquots of respective fractions were analyzed by immunoblotting with the indicated antibodies. PEX13, a PMP; acyl-CoA oxidase (AOx), a peroxisomal matrix enzyme. Of the three components of AOx (A, B, and C), only the B chain is shown. Solid and open arrowheads in A and C indicate unmodified and farnesylated epitope-tagged PEX19, respectively. IP, immunoprecipitation. Bars, 10 µm.

(anti-FLAG agarose beads; Fig. 1 C) and subjected to the import assay. HA-PEX26 was detected in peroxisomes, demonstrating that HA-PEX26 copurified with FLAG-PEX19 was specifically targeted to peroxisomes (Fig. 1 D). Importantly, HA-PEX26 targeted to peroxisomes was resistant to alkaline extraction, thereby suggesting that it was firmly anchored into the membrane (Fig. 1 E). These data clearly demonstrate that PEX26 in the cytosolic PEX19–PEX26 complexes is indeed transported to peroxisomes in semi-intact cells. Collectively, it is most likely that PEX19 forms a complex with PEX26 in the cytosol and maintains it in an import-competent state, thereby assisting its import into peroxisomes.

PEX3-dependent peroxisomal targeting of PEX26

Given that the import of most mitochondrial outer membrane (MOM)–directed and several ER-directed TA proteins seems not to require any specific membrane component (Borgese and Fasana, 2011), it is of particular interest to investigate whether the PEX19-mediated import of PEX26 depends on a membrane component. Because PEX3 and PEX16 were proposed to function as a membrane receptor for PEX19–PMP complexes (Fang et al., 2004; Matsuzono and Fujiki, 2006; Matsuzaki and Fujiki, 2008), we focused on these two PMPs and verified the targeting of PEX26 in PEX3- or PEX16-overexpressing semi-intact cells.

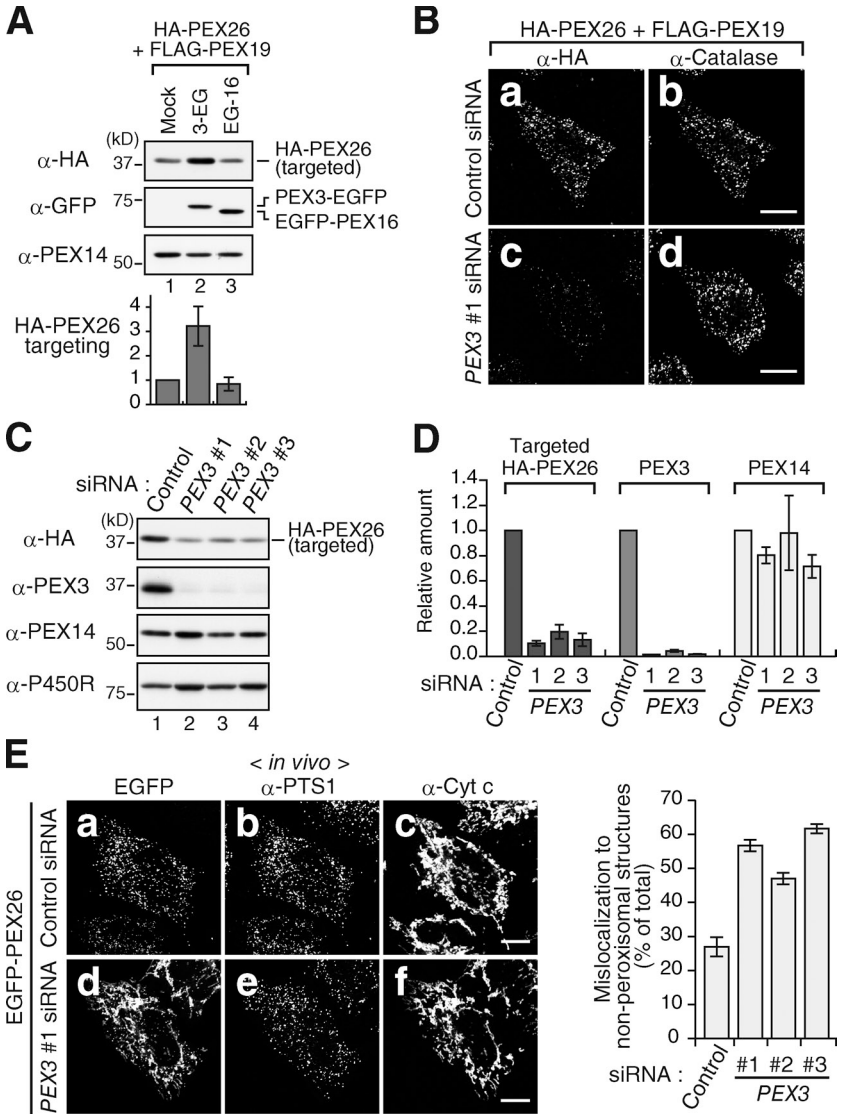

Figure 2. **PEX3 is required for targeting of PEX26.** (A) HeLa cells transfected with empty vector (mock; lane 1), *PEX3-EGFP* (3-EG; lane 2), or *EGFP-PEX16* (EG-16; lane 3) were semipermeabilized and then incubated at 26°C for 1 h with the cytosolic fraction containing FLAG-PEX19 and HA-PEX26. After the import reaction, semi-intact cells were lysed and analyzed by SDS-PAGE and immunoblotting using the indicated antibodies. Targeted HA-PEX26 levels were quantified by densitometry, normalized to PEX14, and shown as ratios to mock-transfected cells (bottom). Values in the graph represent the means ± SD of three independent experiments. (B) HeLa cells were treated with control (a and b) or *PEX3* #1 (c and d) siRNA for 56 h, subjected to in vitro HA-PEX26 import assay as in A, and then immunostained with antibodies against HA and catalase. (C) In vitro HA-PEX26 import assay was likewise performed using semi-intact HeLa cells treated with control siRNA (lane 1) or three different siRNAs against *PEX3* (*PEX3* #1–3; lanes 2–4). Lysates of semi-intact cells were analyzed by immunoblotting using the indicated antibodies. (D) Levels of targeted HA-PEX26 and those of the indicated proteins in C were quantified by densitometry, normalized to cytochrome P450 reductase (P450R), and shown as ratios to control siRNA-treated cells. Data represent the means ± SD of three independent experiments. (E) HeLa cells were treated with control siRNA or three different *PEX3*-specific siRNAs for 44 h and then transfected with *EGFP-PEX26*. After a further 12-h incubation, cells were fixed and immunostained with antibodies to PTS1 and cytochrome *c* (Cyt c). (left) Typical confocal images of control (a–c) and *PEX3* #1 (d–f) siRNA-treated cells. (right) Graph shows percentages of cells exhibiting nonperoxisomal localization of EGFP-PEX26. Data were collected from three independent experiments in which ≥200 cells were scored in each experiment and are represented as the means ± SD. Bars, 10 µm.

After the import reaction, the level of targeted HA-PEX26 was determined by immunoblotting. Results showed that overexpression of PEX3-EGFP, but not EGFP-PEX16, significantly increased the targeting of HA-PEX26 (Fig. 2 A). Conversely, the peroxisomal targeting of HA-PEX26 was markedly compromised in PEX3-depleted semi-intact cells in which the expression level of PEX3 was specifically reduced (Fig. 2, B–D). In line with these results, *PEX3* knockdown gave rise to an increase in mislocalization of newly synthesized EGFP-PEX26 to mitochondria in vivo (Fig. 2 E). Together, these results strongly suggest that peroxisomal targeting of PEX26 depends on PEX3 and that PEX3 functions as a membrane receptor for cytosolic PEX19–PEX26 complexes.

PEX3–PEX19 interaction is essential for peroxisomal targeting of PEX26

PEX3 was shown to interact with PEX19 (Götte et al., 1998; Snyder et al., 1999; Soukupova et al., 1999; Ghaedi et al., 2000; Sacksteder et al., 2000), and the interaction has been proposed to play a prominent role in the biogenesis of peroxisomal membranes, probably by mediating the import of PMPs (Fang et al., 2004; Shibata et al., 2004; Matsuzono et al., 2006; Sato et al., 2008, 2010). Therefore, the role of the PEX3–PEX19 interaction in the peroxisomal targeting of PEX26 was investigated using the in vitro import assay system. A PEX3 mutant harboring a Trp104 to Ala substitution (PEX3-W104A), which is defective in binding to PEX19 (Sato et al., 2008), was first used. Results showed that unlike the wild-type (WT) PEX3, overexpression of PEX3-W104A-EGFP failed to stimulate the targeting of HA-PEX26 in semi-intact cells (Fig. 3 A). This result is interpreted to mean that the PEX3 mutant failed to recruit HA-PEX26. Next, chimeric constructs were generated in which the N-terminal mPTS of PEX3 was replaced by the first 69 amino acid residues of the MOM protein Tom20, which contain its MOM-targeting signal (Kanaji et al., 2000). The chimeric proteins, termed Mito-PEX3-EGFP and Mito-PEX3-W104A-EGFP, were expressed in HeLa cells and subjected to the in vitro HA-PEX26 import assay. As expected, the chimeric proteins were localized to mitochondria (unpublished data). In semi-intact cells expressing Mito-PEX3-EGFP, HA-PEX26 colocalized with Mito-PEX3-EGFP in tubular and/or punctate structures as well as with catalase (Fig. 3 B, a–c), indicating that HA-PEX26 was

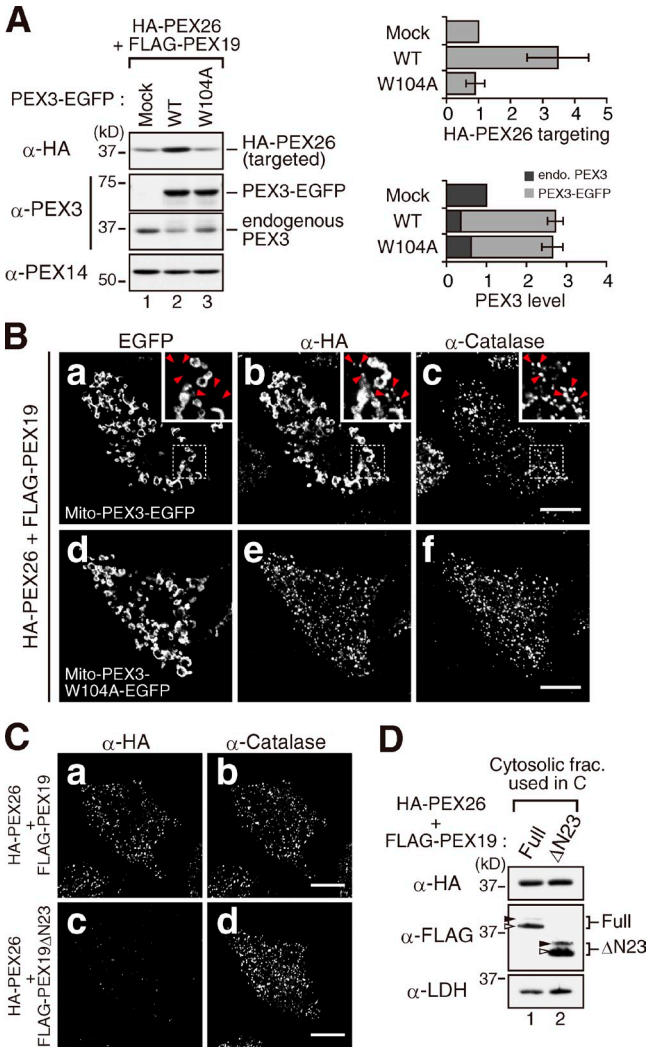

Figure 3. **Peroxisomal targeting of PEX26 is mediated by the PEX3–PEX19 interaction.** (A) In vitro HA-PEX26 import assay was performed as in Fig. 2 A, using semi-intact HeLa cells that had been transfected with empty vector (mock; lane 1), *PEX3-EGFP* (WT; lane 2), or *PEX3-W104A-EGFP* (W104A; lane 3). Lysates of semi-intact cells were subjected to SDS-PAGE and immunoblotting using the indicated antibodies. Levels of targeted HA-PEX26 (top right) and those of PEX3 (bottom right) were determined as in Fig. 2 A. Values are the means ± SD of three independent experiments. Dark and light bars in the bottom graph indicate endogenous (endo.) and exogenous PEX3, respectively. Error bars in the bottom graph are given for total PEX3 levels. (B) Semi-intact HeLa cells expressing Mito-PEX3-EGFP (a–c) or Mito-PEX3-W104A-EGFP (d–f) were subjected to in vitro HA-PEX26 import assay as in Fig. 2 A and then immunostained with antibodies against HA and catalase. Insets show magnified images of the boxed areas. Arrowheads indicate examples of colocalization of HA-PEX26 with catalase. (C) Semi-intact HeLa cells were incubated with the cytosolic fraction containing HA-PEX26 and either FLAG-PEX19 (a and b) or FLAG-PEX19ΔN23 (c and d) and then immunostained as in B. (D) Cytosolic fractions used in C were analyzed by immunoblotting using the indicated antibodies. Full, FLAG-PEX19; ΔN23, FLAG-PEX19ΔN23. Solid and open arrowheads indicate unmodified and farnesylated FLAG-PEX19 (Full and ΔN23), respectively. Bars, 10 μm.

recruited to mitochondria in addition to peroxisomes and supporting the idea that PEX3 functions as a receptor for cytosolic PEX19–PEX26 complexes. In sharp contrast, HA-PEX26 was translocated to peroxisomes in semi-intact cells expressing Mito-PEX3-W104A-EGFP, demonstrating that Mito-PEX3-W104A-EGFP failed to recruit HA-PEX26 to mitochondria (Fig. 3 B, d–f). In agreement with these findings, FLAG-PEX19ΔN23, which is a PEX19 variant lacking the N-terminal 23 amino acid residues and thereby defective in binding to PEX3 (Matsuzono et al., 2006), failed to deliver HA-PEX26 to peroxisomes (Fig. 3, C and D). Of note, PEX19ΔN23 formed soluble complexes with PEX26 as efficiently as WT (Fig. S3). Thus, these data strongly suggest that the import of PEX26 depends on the PEX3–PEX19 interaction and that PEX26 is transported directly from the cytosol to peroxisomes onto PEX3.

ATP and TRC40 are dispensable for the import of PEX26

We next asked whether ATP is required for the targeting and membrane integration of PEX26. EGFP-PEX26 was synthesized in a rabbit reticulocyte lysate (RRL) translation system supplemented with RRL-synthesized HA-PEX19 and then was incubated with semi-intact cells in the presence or absence of apyrase. It should be noted that the addition of RRL-synthesized PEX19 during, but not after, the synthesis of PEX26 resulted in efficient translocation of PEX26 to peroxisomes in semi-intact cells, whereas PEX26 synthesized in the absence of supplemental PEX19 was barely transported to peroxisomes (unpublished data; Pinto et al., 2006). To confirm that ATP is effectively depleted from the import reaction by treatment with apyrase, Myc-Sec61β, a well-defined substrate of TRC40, was synthesized together with EGFP-PEX26 and subjected to the import reaction, and its targeting to the ER was also assessed. As expected, without apyrase (i.e., in the presence of endogenous ATP), EGFP-PEX26 and Myc-Sec61β were transported to peroxisomes and ER-like structures, respectively (Fig. 4 A, top). In contrast, in the presence of apyrase, the import of Myc-Sec61β was almost completely inhibited, whereas peroxisomal targeting of EGFP-PEX26 was observed (Fig. 4 A, bottom). Furthermore, immunoblotting and alkaline extraction showed that the targeting to and integration into the membrane of EGFP-PEX26 were not affected at all by apyrase treatment (Fig. 4 B). These data clearly indicate that neither ATP nor TRC40 is required for the targeting and membrane insertion of PEX26.

Recently, yeast Get3 was shown to interact with the peroxisomal TA protein Pex15p, to mediate the delivery of Pex15p to the ER, and to be required for the peroxisomal localization of Pex15p as well as, to some extent, for the maintenance of functional peroxisomes (Schuldiner et al., 2008; van der Zand et al., 2010). To determine whether TRC40 is involved in the biogenesis of PEX26, the binding of TRC40 to PEX26 was examined. FLAG-tagged Sec61β and PEX26 were synthesized in RRL and subjected to immunoprecipitation under detergent-free conditions. Endogenous TRC40 in RRL was coimmunoprecipitated with FLAG-Sec61β, but not with FLAG-PEX26, thereby indicating that TRC40 did not bind to PEX26 (Fig. 5 A). Moreover, FLAG-PEX26 coincided with cytochrome *c* upon expression in CHO *pex19* ZP119 cells (Kinoshita et al., 1998; Matsuzono et al., 1999), whereas FLAG-Sec61β was colocalized with EGFP targeted to the ER (ER-EGFP; Fig. 5 B). This result suggests that PEX26 is targeted to mitochondria but not to the ER in *PEX19*-deficient mammalian cells where the GET pathway is functional. This is different from the finding that Pex15p is targeted

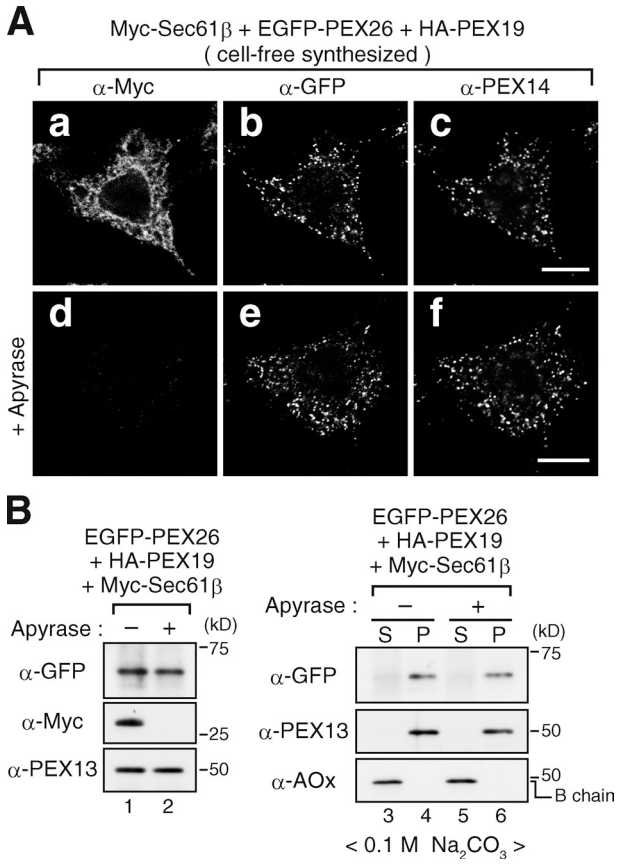

Figure 4. **Pex26 is targeted to and integrated into the peroxisomal membrane in an ATP-independent manner.** (A) Myc-Sec61β and EGFP-PEX26 were synthesized in RRL in the presence of RRL-synthesized HA-PEX19 and then incubated at 26°C for 1 h with semi-intact HeLa cells in the absence (a–c) or presence (d–f) of 5 U/ml apyrase. After fixation, cells were immunostained with antibodies against Myc, GFP, and PEX14. Bars, 10 µm. (B, left) Semi-intact cells shown in A were lysed and analyzed by immunoblotting using the indicated antibodies. (right) Cells shown in A were treated with 0.1 M Na_2CO_3. Soluble (S, supernatant) and membrane (P, pellet) fractions were analyzed by immunoblotting using the indicated antibodies. Of the three components of AOx (A, B, and C), only the B chain is shown.

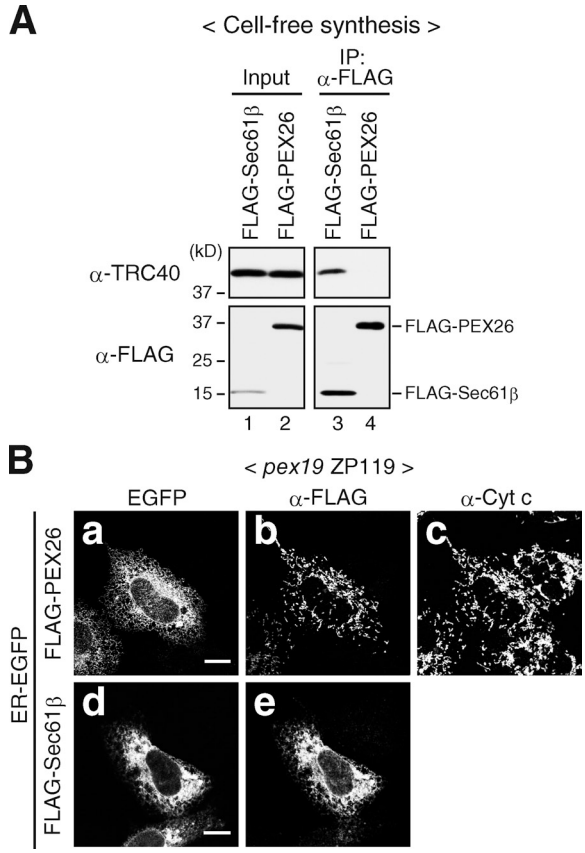

Figure 5. **TRC40 is not involved in the biogenesis of PEX26 in mammalian cells.** (A) FLAG-tagged Sec61β and PEX26 were synthesized in RRL and subsequently subjected to immunoprecipitation (IP) with anti-FLAG agarose beads in detergent-free conditions. Immunoprecipitates and input (10%) were analyzed by SDS-PAGE and immunoblotting using the indicated antibodies. (B) *pex19* ZP119 cells were transfected with *ER-EGFP* together with either *FLAG-PEX26* (a–c) or *FLAG-SEC61β* (d and e). Cells were immunostained with antibodies against FLAG and cytochrome *c* (Cyt c). Bars, 10 µm.

to the ER in *PEX19*-deficient yeast cells (Schuldiner et al., 2008; van der Zand et al., 2010). Collectively, these observations suggest that TRC40 is not involved in the biogenesis of PEX26 in mammalian cells.

Basic amino acid residues in the C segment are essential for peroxisomal targeting of PEX26

Next, we attempted to characterize the signal that directs TA proteins to mammalian peroxisomes. Here, we focused on the basic amino acids within the C segment of PEX26 because (a) the C segment of PEX26 containing a PEX19 binding site is required for the correct targeting of PEX26 (Halbach et al., 2006), (b) basic amino acids are found in the mPTSs of many PMPs (Van Ael and Fransen, 2006), and (c) at least in some cases, the basicity of the C segment determines the subcellular localization of TA proteins in mammalian cells (Borgese and Fasana, 2011).

To assess the importance of basic amino acids in the C segment of PEX26, EGFP-PEX26 variants were generated in which one to four positively charged residues within the luminal PEX19 binding site were replaced by serine residues (termed K1S, RRK3S, and KRRK4S; Fig. 6 A). When WT EGFP-PEX26 was transiently expressed in HeLa cells, it was efficiently localized to peroxisomes, as demonstrated by colocalization with PTS1 proteins (Fig. 6 B, a and b). As noted in the previous section, however, in several cells, WT EGFP-PEX26 was partly localized to mitochondria probably because of overexpression (unpublished data). Upon reduction of the positive charges in the luminal PEX19 binding site, the efficiency of peroxisomal localization was decreased, and conversely, the extent of mitochondrial localization was increased (Fig. 6 B, c–h). These results suggest that positively charged residues in the C segment are essential for peroxisomal targeting of PEX26. Consistent with this finding and the previous study (Halbach et al., 2006), the variant lacking the C segment (ΔCS) was not localized to peroxisomes and was rather localized to mitochondria (Fig. 6 B, i and j). Interestingly, the variant in which only charged residues within the C segment were fused to the region downstream of the TMD (CHARGE) was localized to peroxisomes and partly to mitochondria (Fig. 6 B, k and l), implying that a C-terminal TMD and a following cluster of basic amino acids could function as an mPTS in mammalian cells. Strikingly, the PEX26 variants with

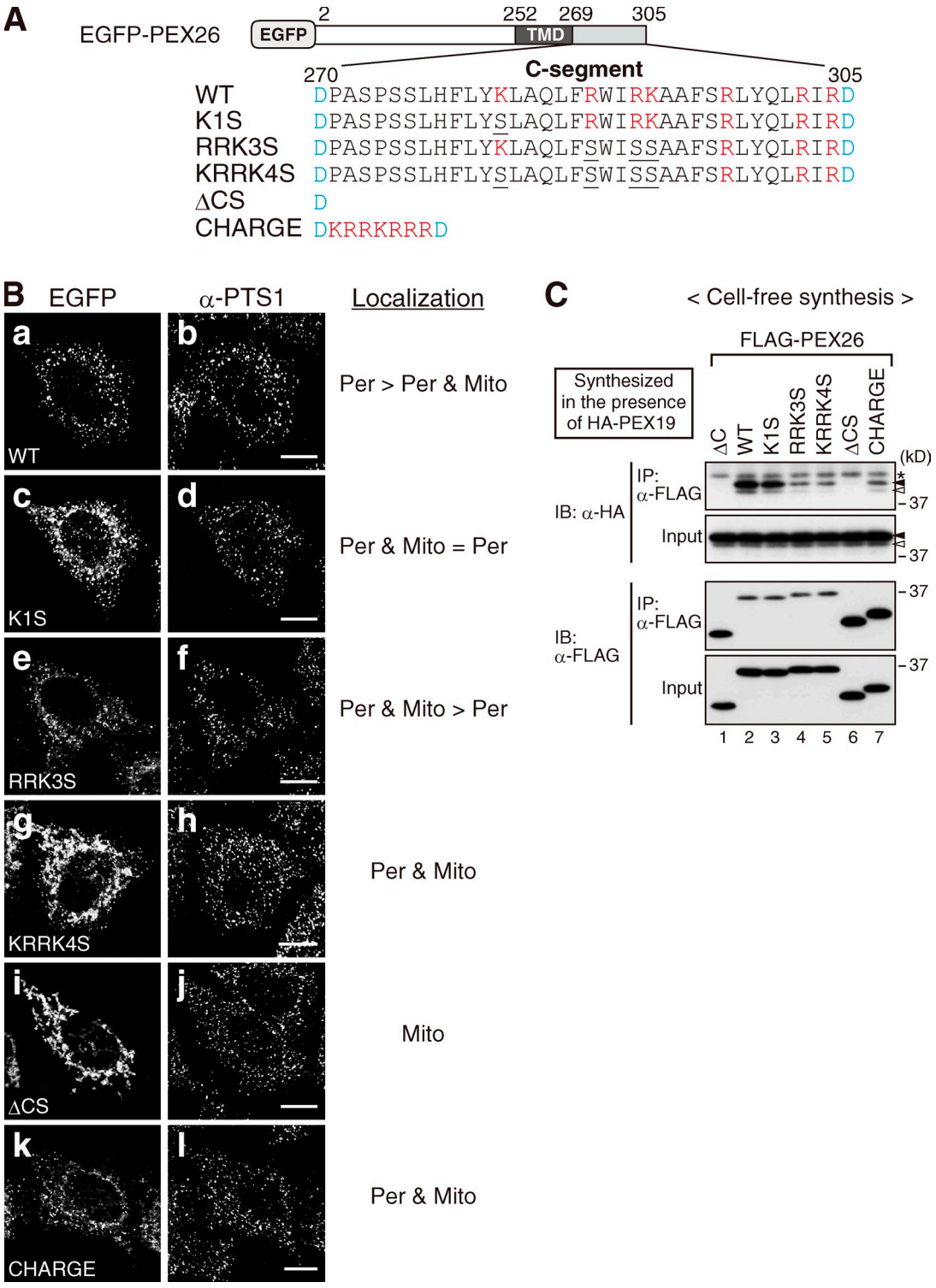

Figure 6. **Basic amino acid residues in the C segment are essential for peroxisomal targeting of PEX26.** (A) Schematic representation of EGFP-PEX26 variants used. Amino acid sequences of the C segment are indicated by the single letter code. Basic and acidic amino acid residues are shown in red and blue letters, respectively, and mutated residues are underlined. (B) HeLa cells transiently expressing the respective EGFP-PEX26 proteins indicated on the left were fixed and then immunostained with the anti-PTS1 antibody. Bars, 10 μm. Intracellular localization of each EGFP-PEX26 protein is shown on the right. Per, peroxisome; Mito, mitochondria; marks (= and >) represent equal frequency and higher frequency, respectively. For instance, the label "Mito & Per > Per" for RRK3S indicates that cells showing both mitochondrial and peroxisomal localization of the EGFP-fused protein were found more frequently than cells showing only peroxisomal localization. (C) FLAG-PEX26 variants indicated at the top were synthesized in RRL in the presence of RRL-synthesized HA-PEX19 and subjected to immunoprecipitation with anti-FLAG agarose beads. Immunoprecipitates (IP) and input (10%) were analyzed by immunoblotting (IB) using the indicated antibodies. Solid and open arrowheads indicate unmodified and farnesylated HA-PEX19, respectively. The asterisk indicates a cross-reactive, nonspecific band.

reduced peroxisomal targeting efficiency, such as RRK3S and KRRK4S, showed reduced binding affinity to PEX19 (Fig. 6 C), suggesting that the reduced peroxisomal targeting efficiency is accounted for by the lower binding affinity to PEX19 and that positively charged residues in the C segment of PEX26 are prerequisite to binding to PEX19.

Basic amino acid residues in the C segment are important, but not sufficient, for peroxisomal targeting of TA proteins

As described in the previous section, the TMD of PEX26 followed by a short cluster of basic amino acids serves as an mPTS (Fig. 6 B), thus raising the possibility that positive charges in the C segment determine the peroxisomal targeting of TA proteins. To assess this possibility, we selected a set of well-known TA proteins (Fig. 7 A; Borgese et al., 2003; Borgese and Fasana, 2011), including EGFP-fused constructs (WT) as well as their variants (R) in which the net positive charge in the C segment was increased to match that of PEX26 (Fig. 7 B, left), and determined their localization in HeLa cells. The WT form of a MOM-destined TA protein, OMP25, was localized to mitochondria, and those of ER-localized TA proteins, cytochrome b_5 (Cyt b_5) and Sec61β, were localized to the reticular ER structures (Fig. 7 B, a, e, and i). The WT vesicular-associated protein 2 (VAMP2), which is transported from the ER to synaptic vesicles in neuronal cells (Kutay et al., 1995), was localized to the plasma membrane and intracellular membranes in HeLa cells (Fig. 7 B, m). Strikingly, the R variants, termed OMP25-R and Cyt b_5-R, were localized to peroxisomes (Fig. 7 B, c, d, g, and h). The aberrant peroxisome morphology observed in OMP25-R–expressing cells might be related to the function of OMP25 in the recruitment of synaptojanin 2A to mitochondria (Nemoto and De Camilli, 1999). In contrast, Sec61β-R and VAMP2-R were not localized to peroxisomes (Fig. 7 B, k, l, o, and p). These findings suggest that the basicity of the C segment is important, but not sufficient, for the peroxisomal localization of TA proteins. Notably, although EGFP–Sec61β-R seemed to be localized to ER-like structures, the pattern of EGFP fluorescence was not the same as that of the corresponding WT protein. For instance, EGFP-Sec61β was localized to the nuclear envelope, but EGFP–Sec61β-R was not (Fig. 7 B, i and k). Thus, the basicity of the C segment may affect the postinsertional sorting of ER-localized TA proteins to a subdomain of the ER.

Next, we investigated whether the peroxisomal targeting of OMP25-R and Cyt b_5-R depends on PEX19. In *PEX19* siRNA-treated cells, EGFP–OMP25-R and EGFP–Cyt b_5-R were detected in both peroxisomes and mitochondria, as assessed by colocalization with PTS1 proteins and cytochrome *c*, respectively (Fig. 7 C and Fig. S4, A and B). These results suggest that *PEX19* knockdown impairs the targeting of OMP25-R and Cyt b_5-R to peroxisomes.

TRC40 interferes with PEX19 in binding to Sec61β-R and VAMP2-R

By increasing the basicity of the C segment, the C-terminal regions of OMP25 and Cyt b_5, but not Sec61β and VAMP2, can be converted into targeting signals for peroxisomes (Fig. 7). To address whether this difference can be explained simply by binding to PEX19, the interaction between PEX19 and the EGFP-fused proteins used in Fig. 7 was examined. Digitonin lysates of HeLa cells overexpressing each of the EGFP-fused proteins together with Myc-PEX19 or FLAG-PEX19 were subjected to immunoprecipitation with anti-FLAG agarose beads followed by immunoblot analysis. All of the R variants were coimmunoprecipitated efficiently and specifically with FLAG-PEX19 (Fig. 8 A), indicating that PEX19 recognized and interacted with not only EGFP–OMP25-R and EGFP–Cyt b_5-R but also EGFP–Sec61β-R and EGFP–VAMP2-R. Furthermore, the amounts of R variants coimmunoprecipitated with FLAG-PEX19 were similar (Fig. S4 C). Therefore, the failure of Sec61β-R and VAMP2-R to localize to peroxisomes is unlikely to be caused by the defect in binding to PEX19. It should be noted that although the efficiency was quite low, a portion of WT EGFP-OMP25, -Sec61β, and -VAMP2 was also coimmunoprecipitated with FLAG-PEX19. The physiological significance of this interaction is unclear; however, this interaction may not occur under physiological conditions because none of the three proteins is targeted to peroxisomes (also see the following paragraph).

An intriguing question remains as to why Sec61β-R and VAMP2-R are destined for the ER but not for peroxisomes, despite the fact that they are recognized by PEX19. Importantly, OMP25 and Cyt b_5 can spontaneously insert into the membrane, whereas both Sec61β and VAMP2 require TRC40 for insertion into the ER membrane (Fig. 7 A). In this context, association of TRC40 with its substrates was shown to depend primarily on TMD hydrophobicity (Mariappan et al., 2010), implying that TRC40 may bind to Sec61β-R and VAMP2-R. Moreover, cytosolic factors other than TRC40, including chaperones and quality control factors, may also interact with them (Abell et al., 2007; Leznicki et al., 2010; Hessa et al., 2011). Therefore, we supposed that under physiological conditions and with endogenous levels of PEX19, PEX19 might have little chance to bind to Sec61β-R and VAMP2-R. To verify this issue, FLAG-tagged proteins were synthesized in RRL and then immunoprecipitated under detergent-free conditions. Endogenous TRC40 in RRL was coimmunoprecipitated with the WT as well as the R forms of Sec61β and VAMP2 but not with PEX26 (Fig. 8 B), thereby demonstrating that TRC40 indeed recognizes and captures the R variants. Notably, the amounts of TRC40 coimmunoprecipitated with the R variants were comparable to those coimmunoprecipitated with the corresponding WT proteins.

A similar result was obtained when these variants were synthesized in the presence of RRL-synthesized HA-PEX19 (Fig. 8 C), implying that the addition of HA-PEX19 did not affect the binding of TRC40 to the R variants. Importantly, Sec61β-R and VAMP2-R did not appear to interact with HA-PEX19 under this experimental condition. First, because anti-FLAG agarose beads nonspecifically adsorbed HA-PEX19 under detergent-free conditions (not depicted), HA-PEX19 was found even in the immunoprecipitates of PEX26ΔC lacking the PEX19-binding domains, though the amount of HA-PEX19 was lower than that in PEX26 immunoprecipitates (Fig. 8 C, lanes 1 and 2). Second, the amounts of HA-PEX19 found in immunoprecipitates of Sec61β and VAMP2 variants were comparable to those

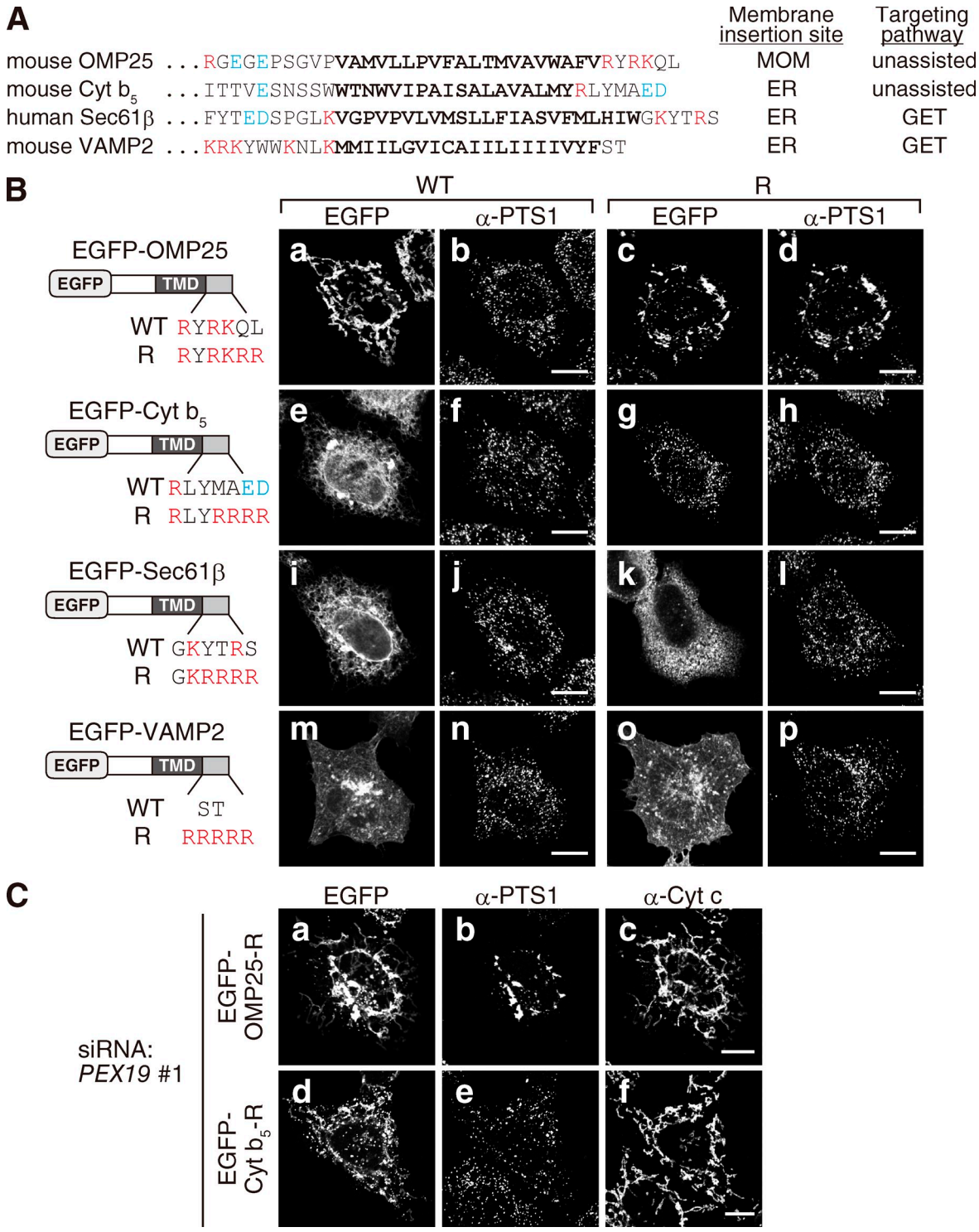

Figure 7. **Basic residues in the C segment are important, but not sufficient, for peroxisomal targeting of TA proteins.** (A) Amino acid sequences of the C-terminal part of several TA proteins and their insertion sites as well as their targeting pathways are shown. The TMDs are bolded, and basic and acidic amino acid residues are shown in red and blue letters, respectively. (B, left) Schematic representation of various EGFP-fused TA proteins (WT) and their variants (R) in which the net positive charge in the C segment was increased. Amino acid sequences of the respective C segments of the proteins are also indicated. (right) The WT and R forms of EGFP-OMP25 (a–d), EGFP–Cyt b_5 (e–h), EGFP-Sec61β (i–l), and EGFP-VAPM2 (m–p) were transiently expressed in HeLa cells and assessed for intracellular localization. EGFP-fused proteins and peroxisomes were detected by EGFP fluorescence and immunostaining with the anti-PTS1 antibody, respectively. (C) HeLa cells were treated with *PEX19* #1 siRNA for 44 h and then transfected with cDNA encoding EGFP–OMP25-R (a–c) or EGFP–Cyt b_5-R (e–f). After a further 12-h incubation, cells were fixed and immunostained with antibodies to PTS1 and cytochrome *c* (Cyt c). Bars, 10 μm.

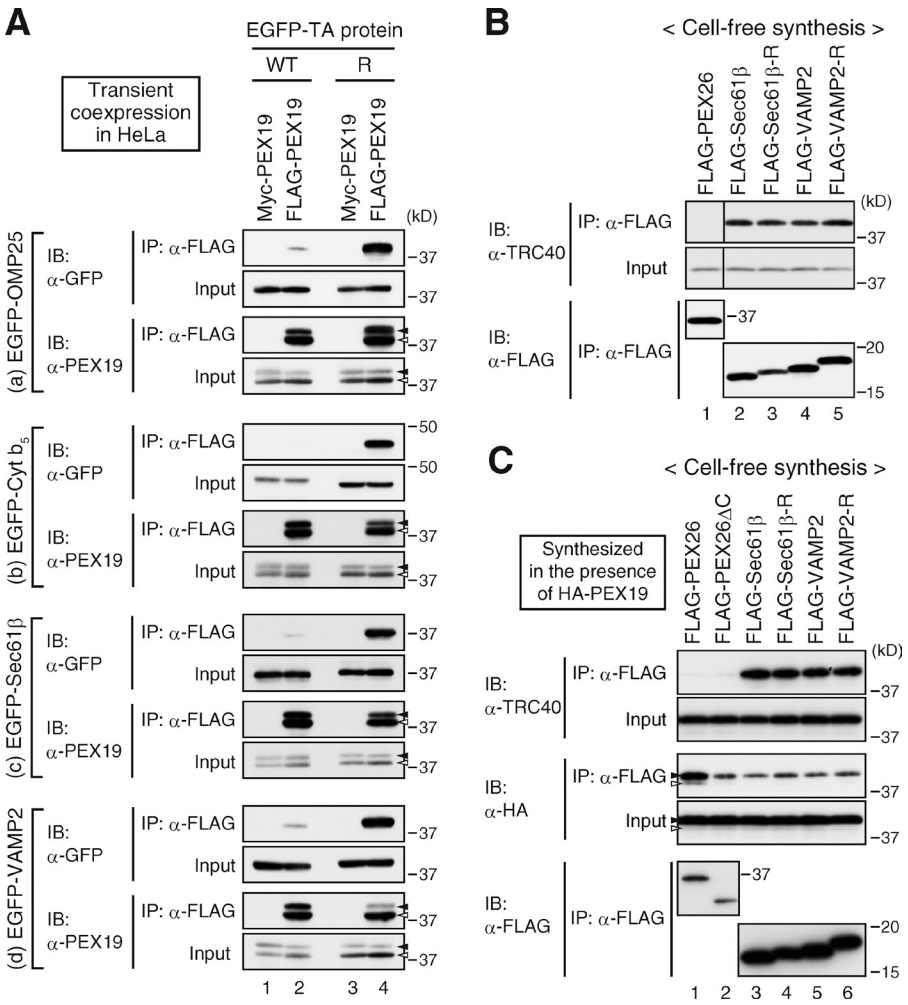

Figure 8. **Capture by TRC40 hinders the potential of PEX19 to interact with Sec61β-R and VAMP2-R.** (A) HeLa cells each transiently expressing EGFP-OMP25 (a), EGFP–Cyt b_5 (b), EGFP-Sec61β (c), and EGFP-VAPM2 (d) proteins (WT, lanes 1 and 2; R, lanes 3 and 4) in combination with Myc-PEX19 or FLAG-PEX19 were lysed and subjected to immunoprecipitation with anti-FLAG agarose beads. Immunoprecipitates and input (10%) were analyzed by SDS-PAGE and immunoblotting with the indicated antibodies. Note that endogenous PEX19 is not visible at this exposure of the blot. (B and C) FLAG-tagged proteins indicated at the top were synthesized in RRL in the absence (B) or presence (C) of RRL-synthesized HA-PEX19 and then immunoprecipitated as in Fig. 5 A. Immunoprecipitates and input (10%) were analyzed by immunoblotting using the indicated antibodies. Solid and open arrowheads indicate unmodified and farnesylated HA-PEX19, respectively. Black line indicates that intervening lanes have been spliced out. IB, immunoblot; IP, immunoprecipitation.

in immunoprecipitates of PEX26ΔC (Fig. 8 C, lanes 2–6). These results are interpreted to mean that Sec61β-R and VAMP2-R are captured by TRC40 and/or possibly by other cytosolic factors, but not PEX19, under physiological conditions, thereby being destined for the ER.

Discussion

Great attention has been paid to the mechanisms underlying the delivery of TA proteins to their target membranes; however, the molecular basis for the import of peroxisomal TA proteins has remained elusive, particularly in mammals.

Peroxisomal import of TA proteins in mammalian cells

The mechanistic details of the PEX19-dependent targeting of PEX26 have yet to be elucidated. The present work demonstrates that (a) PEX19 forms a complex with PEX26 in the cytosol and delivers it to peroxisomes in semi-intact HeLa cells (Fig. 1 and Fig. 3), (b) the peroxisomal import of PEX26 depends on PEX3 and more specifically on the PEX3–PEX19 interaction (Fig. 2 and Fig. 3), and (c) the entire process of PEX26 import is energy independent (Fig. 4). Based on these results, we suggest a PEX19–PEX3-dependent direct import of PEX26, which is further supported by our earlier finding that cell-free synthesized PEX26 is imported into isolated peroxisomes in a PEX19-stimulated manner (Matsuzono and Fujiki, 2006).

The PEX19–PEX3-dependent direct import of PMPs, termed the class I pathway, was first proposed by Fang et al. (2004) and Jones et al. (2004). Most importantly, our results provide the first evidence that PEX3 indeed recruits PMP-loaded PEX19 and thereby mediates the direct import of PMPs. Whether the direct import requires any factors besides PEX3 and PEX19 remains to be defined. Remarkably, the PEX19–PEX26 complex immunoaffinity isolated from the cytosolic fraction of CHO-K1 cells contains the minimal factors required for PEX26 import (Fig. 1, C–E). The mechanistic basis of the membrane insertion also awaits future studies. Given the fact that TA proteins with moderately hydrophobic TMDs can insert spontaneously into protein-free liposomes (Brambillasca et al., 2005, 2006; Kemper et al., 2008), the membrane insertion of PEX26 could occur without assistance from any factors. Biochemical reconstitution studies might provide the answer to these questions.

Meanwhile, the ER to peroxisome trafficking of TA proteins was suggested in yeast and plant cells (Elgersma et al., 1997; Mullen et al., 1999). More recent studies suggest that yeast Pex15p is inserted into the ER via the GET pathway and sorted to peroxisomes via a poorly characterized mechanism

involving yeast Pex19p and ATP (Schuldiner et al., 2008; Jonikas et al., 2009; Costanzo et al., 2010; Lam et al., 2010; van der Zand et al., 2010). We demonstrate that ATP depletion abolishes the import of Sec61β but not that of PEX26 (Fig. 4) and that TRC40 fails to interact with PEX26 (Fig. 5 A). Moreover, the ER localization of PEX26 was not observed even in *pex19* ZP119 cells (Fig. 5 B). These results argue against the involvement of the ER in PEX26 import. Thus, the targeting pathway of peroxisomal TA proteins may not be evolutionarily conserved. Nevertheless, the 1-h incubation used in our in vitro import assay might still leave room for an ER targeting before the peroxisomal targeting. Given that the direct import and ER to peroxisome trafficking pathways are not necessarily mutually exclusive, it is possible that these two pathways might operate simultaneously in one organism and that eukaryotic cells might use either one or both pathways depending on requirements.

In mammalian cells, several TA proteins, including fission1 (Fis1), are found in both mitochondria and peroxisomes (Koch et al., 2005; Kobayashi et al., 2007; Gandre-Babbe and van der Bliek, 2008; Dixit et al., 2010). A recent study suggested that peroxisomal targeting of Fis1 depends on PEX19 (Delille and Schrader, 2008). Hence, the PEX19–PEX3-dependent direct import pathway appears to deliver a small pool of nascent Fis1 to peroxisomes, although this remains to be demonstrated experimentally. The dual localization of Fis1 may be explained by its weak affinity for PEX19. Consistently, PEX26 variants with reduced affinity for PEX19 are indeed targeted to both peroxisomes and mitochondria (Fig. 6). Further studies are required to understand precisely how the dual targeting of Fis1 and the others is achieved and/or regulated.

mPTS of peroxisomal TA proteins

The targeting signal of PEX26 was also analyzed by focusing on the positively charged residues within the luminal PEX19 binding site (Halbach et al., 2006). The positive charges are indeed essential for peroxisomal targeting of PEX26 because a decrease in the positive charges lowers the efficiency of peroxisomal targeting (Fig. 6 B). The impaired peroxisomal targeting appears to mirror the decrease in binding to PEX19 (Fig. 6 C). The peroxisomal localization of PEX26-CHARGE, OMP25-R, and Cyt b_5-R further supports the importance of the positive charges and suggests that a C-terminal TMD with a following short cluster of basic amino acids serves as an mPTS (Fig. 6 B and Fig. 7). Plant peroxisomal ascorbate peroxidase indeed harbors such a short, highly basic C segment, although such a C segment remains to be identified in mammals. Given that a short cluster of basic amino acids does not fit the predicted PEX19 binding motif (Rottensteiner et al., 2004; Halbach et al., 2005), the presence of a PEX19 binding site within the C segment may not be essential for peroxisomal targeting. In the case of PEX26, however, the luminal PEX19 binding site is likely to secure the efficient peroxisomal targeting (Fig. 6 B). The structural analysis of PEX19–PEX26 complexes would address the roles of the two PEX19 binding sites found in PEX26.

A highly basic C segment is important, but not sufficient, for the peroxisomal targeting of TA proteins, as noted for Sec61β-R and VAMP2-R, which are not localized to peroxisomes and rather are destined for the ER (Fig. 7). Surprisingly, PEX19 interacts with Sec61β-R and VAMP2-R under conditions of overexpression and detergent solubilization (Fig. 8 A). However, it is most likely that under physiological conditions, Sec61β-R and VAMP2-R are captured by TRC40, not PEX19 (Fig. 8, B and C), in accordance with the fact that the association of TRC40 with its substrate depends primarily on TMD hydrophobicity (Mariappan et al., 2010). Collectively, our results suggest that TA proteins that not only interact with PEX19 but also escape from capture by TRC40 are targeted to peroxisomes. Peroxisomal TA proteins would therefore require a less hydrophobic TMD to avoid capture by TRC40 and require a highly basic C segment to ensure binding to PEX19.

Selective targeting of TA proteins to the correct membranes in mammalian cells

Recent studies, including ours, have uncovered the targeting pathways of TA proteins in mammalian cells: the GET pathway for most ER-destined TA proteins (Stefanovic and Hegde, 2007), the PEX19–PEX3-dependent pathway for peroxisomal TA proteins (this study; Halbach et al., 2006), and the unassisted pathways for several ER-destined and most, if not all, MOM-targeted TA proteins (Brambillasca et al., 2005; Setoguchi et al., 2006; Kemper et al., 2008; Colombo et al., 2009). To achieve selective targeting, newly synthesized TA proteins must be sorted to the appropriate targeting pathway. Sec61β-R and VAMP2-R, showing significant affinity to PEX19, are captured by TRC40 and destined for the ER (Fig. 7 and Fig. 8), thereby suggesting that the GET pathway outcompetes the PEX19–PEX3-dependent pathway. Given that the GET pathway (a) appears to thoroughly hinder the potential targeting of ER-destined TA proteins to mitochondria (Schuldiner et al., 2008; Jonikas et al., 2009) and (b) succeeds in substrate loading onto TRC40 despite the presence of competing cytosolic factors (Mariappan et al., 2010), it is more likely that the GET pathway can uptake ER-destined TA proteins before other targeting pathways gain access to them (Fig. 9). Notably, the substrate recognition by the GET pathway seems to begin before the TMDs of TA proteins emerge from ribosomes (Mariappan et al., 2010).

TA protein sorting in several targeting pathways is likely dictated by a combination of substrate properties and availability of binding partners. With respect to substrate features, TMD hydrophobicity is possibly a key determinant for the access to, or exclusion from, the GET pathway (Borgese et al., 2007; Rabu et al., 2008; Mariappan et al., 2010). TA proteins excluded from the GET pathway are more likely to be sorted based on C-terminal basicity (Fig. 9; this study; Isenmann et al., 1998; Kuroda et al., 1998; Borgese et al., 2001; Horie et al., 2002; Kaufmann et al., 2003); however, as there is some overlap in the hydrophobicity and basicity between TA proteins (Borgese et al., 2007), further biochemical and structural studies using a large number of bona fide and artificial sequences are required to envisage how each targeting pathway discriminates specific substrates from closely related TA substrates. Moreover, it should be also clarified whether and how the activities of the components of each targeting pathway are regulated. Addressing these issues should lead to a comprehensive understanding of the selective targeting of TA proteins.

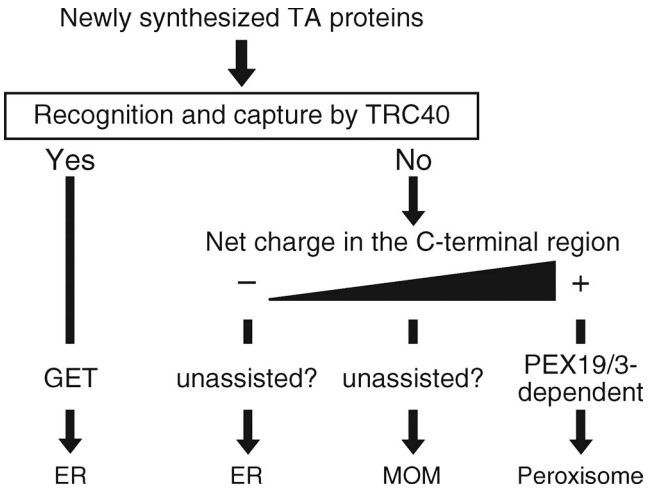

Figure 9. **A model for selective targeting of TA proteins in mammalian cells.** TA proteins are suggested to be sorted by any of several targeting pathways. Upon synthesis, TA proteins harboring a TMD suitable for association with TRC40 are trapped in the GET pathway and delivered to the ER. TA proteins excluded from the GET pathway are then sorted according to the C-terminal basic charge: those highly positive are delivered via the PEX19–PEX3-dependent pathway to peroxisomes, and those with moderate and low basicity are targeted via the unassisted pathway to the MOM and the ER, respectively.

Materials and methods

Antibodies

Rabbit antibodies to acyl-CoA oxidase (AOx; raised against full-length rat AOx; Tsukamoto et al., 1990), catalase (raised against full-length human catalase; Shimozawa et al., 1992), PTS1 peptide (raised against aa 652–661 of rat AOx; Otera et al., 1998), PEX3 (raised against aa 356–373 of human PEX3; Ghaedi et al., 2000), PEX13 (raised against aa 256–403 of human PEX13; Mukai and Fujiki, 2006), PEX14 (raised against aa 358–376 of rat PEX14; Shimizu et al., 1999), HA (raised against HA epitope [YPYDVPDYA]; Otera et al., 2000), and guinea pig anti-PEX14 antibody (raised against aa 241–376 of rat PEX14; Mukai et al., 2002) were described previously. Rabbit anti-TRC40 antibody (raised against full-length human TRC40; Mariappan et al., 2010) was a gift from R.S. Hegde (Medical Research Council Laboratory of Molecular Biology, Cambridge, England, UK). The following primary antibodies were purchased from the indicated vendors: rabbit antibodies against FLAG (Sigma-Aldrich) and GFP (Medical and Biological Laboratories); mouse monoclonal antibodies against FLAG (M2; Sigma-Aldrich), HA (16B12; Covance), c-Myc (9E10; Santa Cruz Biotechnology, Inc.), GFP (B-2; Santa Cruz Biotechnology, Inc.), cytochrome P450 reductase (F-10; Santa Cruz Biotechnology, Inc.), cytochrome *c* (BD), PEX19 (BD), and α-tubulin (Abcam); and goat anti–lactate dehydrogenase antibody (Rockland Immunochemicals). Secondary antibodies used for immunoblotting were HRP-linked sheep anti–mouse IgG, donkey anti–rabbit IgG (GE Healthcare), and rabbit anti–goat IgG (Invitrogen) antibodies. Secondary antibodies for immunostaining included Alexa Fluor 488–, 568–, or 647–conjugated goat anti–mouse IgG and anti–rabbit IgG antibodies and Alexa Fluor 647–conjugated goat anti–guinea pig IgG antibody (Invitrogen).

Cell culture, DNA transfection, and RNAi

CHO cells, including CHO-K1 and CHO *pex19* ZP119 (Kinoshita et al., 1998; Matsuzono et al., 1999), were maintained in Ham's F-12 medium (Invitrogen) supplemented with 10% FBS, and HeLa cells were maintained in DMEM (Invitrogen) supplemented with 10% FBS. All cell lines were cultured at 37°C under 5% CO_2. DNA transfections were performed using Lipofectamine 2000 (Invitrogen) for HeLa cells and Lipofectamine reagent (Invitrogen) for CHO cells according to the manufacturer's instructions. siRNA-mediated knockdown of *PEX3* and *PEX19* in HeLa cells was performed using predesigned Stealth RNAi siRNAs (Invitrogen) with Stealth RNAi Negative Control Medium GC Duplex (Invitrogen) as a control. The sequences of siRNAs are listed in Table 1. HeLa cells were transfected twice at a 24-h interval with 33 nM siRNA duplexes using Lipofectamine 2000.

Plasmids

All plasmids used in this study (Table 2) were constructed by standard methods and verified by DNA sequencing. The cDNAs encoding human PEX26, human PEX19, rat PEX3, and EGFP were amplified by PCR from pCMVSPORT/*PEX26* (Matsumoto et al., 2003), pUcD2Hyg/HA_2-*PEX19* (Matsuzono et al., 2006), pcDNAZeo/*RnPEX3* (Ghaedi et al., 2000), and pEGFP vector (Takara Bio Inc.), respectively. The cDNAs encoding human Sec61β, human Hsp47, mouse OMP25, mouse Cyt b_5, mouse VAMP2, and rat Tom20 were obtained by RT-PCR using total RNA isolated from HeLa cells, mouse brain tissue, and rat liver tissue, respectively.

The cDNAs encoding full-length PEX26, PEX26ΔC (aa 2–246), and PEX26ΔCS (aa 2–270) were PCR amplified and cloned into a modified pcDNA3.1/Zeo(+) vector (Invitrogen) encoding an N-terminal FLAG tag (pcDNAZeo/*FLAG*) or EGFP (pcDNAZeo/*EGFP*) via the BamHI–NotI sites. The cDNA coding for full-length PEX26 was also cloned into a modified pcDNA3.1/Zeo(+) vector encoding an N-terminal 2×HA tag. The cDNAs encoding PEX26-K1S, PEX26-RRK3S, and PEX26-KRRK4S were generated by overlap extension PCR (Ho et al., 1989) and ligated into the BamHI–NotI sites of pcDNAZeo/*FLAG* and pcDNAZeo/*EGFP*. The cDNAs encoding PEX26-CHARGE, OMP25, OMP25-R, Cyt b_5, Cyt b_5-R, Sec61β, Sec61β-R, VAMP2, and VAMP2-R were cloned into the BamHI–XhoI sites of pcDNAZeo/*FLAG* and pcDNAZeo/*EGFP*. The cDNA coding for Sec61β was also cloned into a modified pcDNA3.1/Zeo(+) vector encoding an N-terminal 6×Myc tag.

The cDNAs encoding PEX19 and PEX19ΔN23 (aa 24–299) were cloned into the BamHI–XhoI sites of pcDNAZeo/*FLAG* and a modified pcDNA3.1/Zeo(+) vector encoding an N-terminal Myc tag. The cDNA coding for full-length rat PEX3 was cloned into the BamHI–XhoI sites of pcDNAZeo/*C-EGFP*, a modified pcDNA3.1/Zeo(+) vector encoding a C-terminal EGFP. The cDNA encoding a fusion of aa 1–69 of rat Tom20 and aa 40–373 of rat PEX3 was generated by overlap extension PCR (Horton et al., 1989) and ligated into the BamHI–XhoI sites of pcDNAZeo/*C-EGFP*, yielding pcDNAZeo/*Mito-PEX3-EGFP*. For pcDNAZeo/*PEX3-W104A-EGFP* and pcDNAZeo/*Mito-PEX3-W104A-EGFP*, the W104A

Table 1. **Sequences of siRNAs used in this study**

Code	Strand	Sequence
Human *PEX19* #1	Sense	5′-AGAAUGGUUGCAGAGUCAUCGGGAA-3′
	Antisense	5′-UUCCCGAUGACUCUGCAACCAUUCU-3′
Human *PEX19* #2	Sense	5′-GGAGCUUCUGGAAAGUGCUCUUGAU-3′
	Antisense	5′-AUCAAGAGCACUUUCCAGAAGCUCC-3′
Human *PEX19* #3	Sense	5′-GCCAGUGGUGAACAGUGUCUGAUCA-3′
	Antisense	5′-UGAUCAGACACUGUUCACCACUGGC-3′
Human *PEX3* #1	Sense	5′-GGGAGGAUCUGAAGAUAAUAAGUUU-3′
	Antisense	5′-AAACUUAUUAUCUUCAGAUCCUCCC-3′
Human *PEX3* #2	Sense	5′-UAUUUACCUGGAUAAUGCAGCAGUU-3′
	Antisense	5′-AACUGCUGCAUUAUCCAGGUAAAUA-3′
Human *PEX3* #3	Sense	5′-UCCUCGAGACAUUACCACUAUUAAA-3′
	Antisense	5′-UUUAAUAGUGGUAAUGUCUCGAGGA-3′

mutation was introduced by overlap extension PCR. To generate pcDNAZeo/*ER-EGFP*, the cDNA encoding aa 1–414 of human Hsp47 was ligated into the NheI–BamHI sites of the pcDNA3.1/Zeo(+) vector in which a BamHI–SpeI fragment encoding EGFP followed by a KDEL retention signal had been inserted into the BamHI–XbaI sites. pcDNAZeo/*HA-PEX19* (Matsuzono et al., 2006) and pEGFP-C1/*EGFP-PEX16* (Matsuzaki and Fujiki, 2008) were as described previously.

Immunoblotting

Immunoblotting was performed as described previously (Otera et al., 2000). In brief, protein samples were separated by SDS-PAGE and electrotransferred to a polyvinylidene fluoride membrane (Bio-Rad Laboratories). After blocking in PBS containing 5% nonfat dry milk and 0.1% Tween 20, blots were probed with appropriate primary and HRP-conjugated secondary antibodies, developed with ECL Western blotting detection reagents (GE Healthcare), and exposed to an x-ray film (Hyperfilm ECL; GE Healthcare). For densitometric analysis, immunoblot films were scanned in translucent mode with a scanner (GT-X900; Epson), and the intensity of protein bands was analyzed using the gel analysis tool in ImageJ software (National Institutes of Health). The relative amounts of proteins were determined as described in the figure legends.

Immunofluorescence microscopy

Cells on glass coverslips were fixed with 4% PFA in PBS for 15 min at RT, permeabilized with 1% Triton X-100 in PBS for 5 min at RT, and blocked with PBS-BSA (PBS containing 1% BSA) for 30 min at RT. Subsequently, cells were incubated for 60–90 min at RT with primary antibodies diluted in PBS-BSA, washed extensively with PBS, and incubated for 45 min at RT with appropriate Alexa Fluor 488–, 568–, or 647–conjugated secondary antibodies diluted in PBS-BSA. After extensive washing with PBS, coverslips were rinsed with ultrapure water and mounted on slides with aqueous mounting medium (PermaFluor; Thermo Fisher Scientific). Images were acquired

Table 2. **Plasmids used in this study**

Name	Expressed protein	Reference
pcDNAZeo/*HA-PEX26*	Full-length human PEX26 with an N-terminal 2×HA tag	This study
pcDNAZeo/*FLAG-PEX26*	Full-length human PEX26 with an N-terminal FLAG tag	This study
pcDNAZeo/*FLAG-PEX26ΔC*	PEX26ΔC (aa 2–246) with an N-terminal FLAG tag	This study
pcDNAZeo/*FLAG-PEX26ΔCS*	PEX26ΔCS (aa 2–270) with an N-terminal FLAG tag	This study
pcDNAZeo/*FLAG-PEX26-K1S*	PEX26-K1S (Fig. 6) with an N-terminal FLAG tag	This study
pcDNAZeo/*FLAG-PEX26-RRK3S*	PEX26-RRK3S (Fig. 6) with an N-terminal FLAG tag	This study
pcDNAZeo/*FLAG-PEX26-KRRK4S*	PEX26-KRRK4S (Fig. 6) with an N-terminal FLAG tag	This study
pcDNAZeo/*FLAG-PEX26-CHARGE*	PEX26-CHARGE (Fig. 6) with an N-terminal FLAG tag	This study
pcDNAZeo/*EGFP-PEX26*	Full-length human PEX26 with an N-terminal EGFP	This study
pcDNAZeo/*EGFP-PEX26ΔCS*	PEX26ΔCS with an N-terminal EGFP	This study
pcDNAZeo/*EGFP-PEX26-K1S*	PEX26-K1S with an N-terminal EGFP	This study
pcDNAZeo/*EGFP-PEX26-RRK3S*	PEX26-RRK3S with an N-terminal EGFP	This study
pcDNAZeo/*EGFP-PEX26-KRRK4S*	PEX26-KRRK4S with an N-terminal EGFP	This study
pcDNAZeo/*EGFP-PEX26-CHARGE*	PEX26-CHARGE with an N-terminal EGFP	This study
pcDNAZeo/*EGFP-OMP25*	Full-length mouse OMP25 with an N-terminal EGFP	This study
pcDNAZeo/*EGFP-Cyt b_5*	Full-length mouse Cyt b_5 with an N-terminal EGFP	This study
pcDNAZeo/*EGFP-Sec61β*	Full-length human Sec61β with an N-terminal EGFP	This study
pcDNAZeo/*EGFP-VAMP2*	Full-length mouse VAMP2 with an N-terminal EGFP	This study
pcDNAZeo/*EGFP–OMP25-R*	OMP25-R (Fig. 7) with an N-terminal EGFP	This study
pcDNAZeo/*EGFP–Cyt b_5-R*	Cyt b_5-R (Fig. 7) with an N-terminal EGFP	This study
pcDNAZeo/*EGFP–Sec61β-R*	Sec61β-R (Fig. 7) with an N-terminal EGFP	This study
pcDNAZeo/*EGFP–VAMP2-R*	VAMP2-R (Fig. 7) with an N-terminal EGFP	This study
pcDNAZeo/*FLAG-OMP25*	Full-length mouse OMP25 with an N-terminal FLAG tag	This study
pcDNAZeo/*FLAG-Cyt b_5*	Full-length mouse Cyt b_5 with an N-terminal FLAG tag	This study
pcDNAZeo/*FLAG-Sec61β*	Full-length human Sec61β with an N-terminal FLAG tag	This study
pcDNAZeo/*FLAG-VAMP2*	Full-length mouse VAMP2 with an N-terminal FLAG tag	This study
pcDNAZeo/*FLAG–Sec61β-R*	Sec61β-R with an N-terminal FLAG tag	This study
pcDNAZeo/*FLAG–VAMP2-R*	VAMP2-R with an N-terminal FLAG tag	This study
pcDNAZeo/*Myc-Sec61*	Full-length human Sec61β with an N-terminal 6×Myc tag	This study
pcDNAZeo/*HA-PEX19*	Full-length human PEX19 with an N-terminal 2×HA tag	Matsuzono et al., 2006
pcDNAZeo/*FLAG-PEX19*	Full-length human PEX19 with an N-terminal FLAG tag	This study
pcDNAZeo/*FLAG-PEX19ΔN23*	PEX19ΔN23 (aa 24–299) with an N-terminal FLAG tag	This study
pcDNAZeo/*Myc-PEX19*	Full-length human PEX19 with an N-terminal Myc tag	This study
pcDNAZeo/*Myc-PEX19ΔN23*	PEX19ΔN23 with an N-terminal Myc tag	This study
pcDNAZeo/*PEX3-EGFP*	Full-length rat PEX3 with a C-terminal EGFP	This study
pcDNAZeo/*PEX3-W104A-EGFP*	PEX3 carrying the W104A mutation with a C-terminal EGFP	This study
pcDNAZeo/*Mito-PEX3-EGFP*	A chimeric protein, termed Mito-PEX3-EGFP, comprising aa 1–69 of rat Tom20, aa 40–373 of rat PEX3, and EGFP	This study
pcDNAZeo/*Mito-PEX3-W104A-EGFP*	Identical to Mito-PEX3-EGFP except that PEX3 in this construct harbors the W104A mutation	This study
pcDNAZeo/*ER-EGFP*	A fusion protein comprising aa 1–414 of human Hsp47, EGFP, and a KDEL retention signal	This study
pEGFP-C1/*EGFP-PEX16*	Full-length human PEX16 with an N-terminal EGFP	Matsuzaki and Fujiki, 2008

pEGFP-C1/*EGFP-PEX16* is based on pEGFP-C1 (Takara Bio Inc.), whereas other plasmids are based on pcDNA3.1/Zeo(+) (Invitrogen).

at RT using a laser-scanning confocal microscope (LSM 710 with Axio Observer.Z1; Carl Zeiss) equipped with a 100×/1.46 NA α Plan-Apochromat oil immersion objective and the ZEN 2009 acquisition software (Carl Zeiss). Image contrast and brightness were adjusted in Photoshop CS4 (Adobe).

In vitro import assay using semi-intact HeLa cells

HeLa cells were semipermeabilized as described previously (Matsuzaki and Fujiki, 2008) using 50 µg/ml digitonin in buffer S (0.25 M sucrose, 20 mM Hepes-KOH, pH 7.4, 2.5 mM magnesium acetate, 25 mM KCl, 2.5 mM EGTA, 1 mM DTT, and protease inhibitor cocktail [5 µg/ml aprotinin and 10 µg/ml each of antipain, chymostatin, E-64, leupeptin, and pepstatin]). Semi-intact HeLa cells were incubated for 60 min at 26°C with cytosolic fractions containing epitope-tagged PEX19 and PEX26, immunoaffinity-purified PEX19–PEX26 complexes, or in vitro–synthesized proteins in buffer S. To deplete ATP from the import reactions, 5 U/ml apyrase (Sigma-Aldrich) was added to the reactions. After extensive washing, cells were either fixed for immunofluorescence microscopy or lysed for immunoblot analysis. For alkaline extraction (Fujiki et al., 1982), cells were treated with 0.1 M Na_2CO_3 on ice for 30 min, and soluble and membrane fractions were separated by ultracentrifugation at 100,000 *g* for 30 min.

Subcellular fractionation

CHO-K1 cells expressing epitope-tagged PEX19 and PEX26 were collected in buffer H (0.25 M sucrose, 20 mM Hepes-KOH, pH 7.4, 1 mM EDTA, and protease inhibitor cocktail) and homogenized by passing through a 27-gauge needle (with 1-ml syringe) on ice. Homogenates were centrifuged at 800 *g* for 5 min to yield a postnuclear supernatant. The postnuclear supernatant was then separated into cytosolic and organelle fractions by ultracentrifugation at 100,000 *g* for 30 min. Cytosolic fractions used in the in vitro import assays were prepared in a similar manner using buffer S.

Cell-free synthesis of proteins

In vitro transcription/translation reactions in RRL were performed using the quick coupled transcription/translation system (TnT T7; Promega) according to the manufacturer's instructions. Where indicated, reaction mixtures were supplemented with the in vitro transcription/translation product of *PEX19* to synthesize proteins in the presence of PEX19. The volume of *PEX19* transcription/translation product added was 5–15% (typically 7%) of the final reaction volume, which was suitable for the reconstitution of efficient peroxisomal targeting of cell-free synthesized PEX26 in semi-intact HeLa cells. Samples were cleared by centrifugation at 100,000 *g* for 30 min before use in the immunoprecipitation and in vitro import assays.

Immunoprecipitations

Immunoprecipitation from cytosolic fractions was performed after dilution with an equal volume of buffer C2 (0.2% CHAPS, 20 mM Hepes-KOH, pH 7.4, 300 mM KCl, 1 mM EDTA, 2 mM DTT, 20% glycerol, and protease inhibitor cocktail) using anti-FLAG agarose beads (Sigma-Aldrich). After extensive washing with buffer C (0.1% CHAPS, 20 mM Hepes-KOH, pH 7.4, 150 mM KCl, 1 mM EDTA, 1 mM DTT, 10% glycerol, and protease inhibitor cocktail), proteins bound to the anti-FLAG agarose beads were analyzed by SDS-PAGE and immunoblotting. To prepare immunoaffinity-purified FLAG-PEX19–HA-PEX26 complexes for use in the in vitro import assay, the anti-FLAG agarose beads were further washed with buffer S, and immunoprecipitates were eluted with 100 µg/ml FLAG peptide (Sigma-Aldrich) in buffer S. Where indicated, immunoprecipitation was performed similarly using protein A–Sepharose beads (GE Healthcare) and rabbit anti-HA antibody or preimmune serum.

Immunoprecipitation assays were also performed using cell-free synthesized proteins. Unless otherwise indicated, translation products were subjected to immunoprecipitation with anti-FLAG agarose beads after dilution with buffer C. For immunoprecipitation under detergent-free conditions, translation products were diluted with buffer P (20 mM Hepes-KOH, pH 7.4, 100 mM potassium acetate, 2 mM magnesium acetate, and protease inhibitor cocktail) and then incubated with anti-FLAG agarose beads. After extensive washing with buffer P, the beads were further washed with buffer P containing 250 mM potassium acetate. Immunoprecipitates were subjected to SDS-PAGE and subsequent immunoblotting.

For immunoprecipitation from cell lysates, HeLa cells expressing epitope-tagged PEX19, and EGFP-fused TA proteins were lysed in buffer D (1% digitonin, 20 mM Hepes-KOH, pH 7.4, 150 mM KCl, 1 mM EDTA, 1 mM DTT, 10% glycerol, and protease inhibitor cocktail). Cell lysates were cleared by centrifugation and incubated with anti-FLAG agarose beads. After extensive washing with buffer D, bound proteins were analyzed by SDS-PAGE and immunoblotting.

Online supplemental material

Fig. S1 demonstrates that *PEX19* knockdown impairs peroxisomal targeting of newly synthesized PEX26. Fig. S2 shows that the C-terminal region of PEX26 is required for binding to PEX19. Fig. S3 shows the interaction between PEX19ΔN23 and PEX26 in the cytosol. Fig. S4 shows that peroxisomal targeting of EGFP–OMP25-R and EGFP–Cyt b_5-R depends on PEX19 and also shows the interaction of PEX19 with EGFP-fused OMP25-R, Cyt b_5-R, Sec61β-R, and VAMP2-R. Online supplemental material is available at http://www.jcb.org/cgi/content/full/jcb.201211077/DC1.

We thank R.S. Hegde for the rabbit anti-TRC40 antibody. We also thank M. Nishi and K. Shimizu for figure illustrations and the other members of our laboratory for discussions.

This work was supported in part by a Core Research for Evolutional Science and Technology grant (to Y. Fujiki) from the Science and Technology Agency of Japan, by Grants-in-Aid for Scientific Research, 19058011, 20370039, and 24247038 (to Y. Fujiki), the Global Center of Excellence Program and Grants for Excellent Graduate Schools from the Ministry of Education, Culture, Sports, Science and Technology of Japan, and by grants from the Japan Foundation for Applied Enzymology and the Takeda Science Foundation.

Submitted: 13 November 2012
Accepted: 1 February 2013

References

Abell, B.M., C. Rabu, P. Leznicki, J.C. Young, and S. High. 2007. Post-translational integration of tail-anchored proteins is facilitated by defined molecular chaperones. *J. Cell Sci.* 120:1743–1751. http://dx.doi.org/10.1242/jcs.002410

Borgese, N., and E. Fasana. 2011. Targeting pathways of C-tail-anchored proteins. *Biochim. Biophys. Acta.* 1808:937–946. http://dx.doi.org/10.1016/j.bbamem.2010.07.010

Borgese, N., I. Gazzoni, M. Barberi, S. Colombo, and E. Pedrazzini. 2001. Targeting of a tail-anchored protein to endoplasmic reticulum and mitochondrial outer membrane by independent but competing pathways. *Mol. Biol. Cell.* 12:2482–2496.

Borgese, N., S. Colombo, and E. Pedrazzini. 2003. The tale of tail-anchored proteins: coming from the cytosol and looking for a membrane. *J. Cell Biol.* 161:1013–1019. http://dx.doi.org/10.1083/jcb.200303069

Borgese, N., S. Brambillasca, and S. Colombo. 2007. How tails guide tail-anchored proteins to their destinations. *Curr. Opin. Cell Biol.* 19:368–375. http://dx.doi.org/10.1016/j.ceb.2007.04.019

Brambillasca, S., M. Yabal, P. Soffientini, S. Stefanovic, M. Makarow, R.S. Hegde, and N. Borgese. 2005. Transmembrane topogenesis of a tail-anchored protein is modulated by membrane lipid composition. *EMBO J.* 24:2533–2542. http://dx.doi.org/10.1038/sj.emboj.7600730

Brambillasca, S., M. Yabal, M. Makarow, and N. Borgese. 2006. Unassisted translocation of large polypeptide domains across phospholipid bilayers. *J. Cell Biol.* 175:767–777. http://dx.doi.org/10.1083/jcb.200608101

Colombo, S.F., R. Longhi, and N. Borgese. 2009. The role of cytosolic proteins in the insertion of tail-anchored proteins into phospholipid bilayers. *J. Cell Sci.* 122:2383–2392. http://dx.doi.org/10.1242/jcs.049460

Costanzo, M., A. Baryshnikova, J. Bellay, Y. Kim, E.D. Spear, C.S. Sevier, H. Ding, J.L. Koh, K. Toufighi, S. Mostafavi, et al. 2010. The genetic landscape of a cell. *Science.* 327:425–431. http://dx.doi.org/10.1126/science.1180823

Delille, H.K., and M. Schrader. 2008. Targeting of hFis1 to peroxisomes is mediated by Pex19p. *J. Biol. Chem.* 283:31107–31115. http://dx.doi.org/10.1074/jbc.M803332200

Dixit, E., S. Boulant, Y. Zhang, A.S. Lee, C. Odendall, B. Shum, N. Hacohen, Z.J. Chen, S.P. Whelan, M. Fransen, et al. 2010. Peroxisomes are signaling platforms for antiviral innate immunity. *Cell.* 141:668–681. http://dx.doi.org/10.1016/j.cell.2010.04.018

Elgersma, Y., L. Kwast, M. van den Berg, W.B. Snyder, B. Distel, S. Subramani, and H.F. Tabak. 1997. Overexpression of Pex15p, a phosphorylated peroxisomal integral membrane protein required for peroxisome assembly in *S. cerevisiae*, causes proliferation of the endoplasmic reticulum membrane. *EMBO J.* 16:7326–7341. http://dx.doi.org/10.1093/emboj/16.24.7326

Fang, Y., J.C. Morrell, J.M. Jones, and S.J. Gould. 2004. PEX3 functions as a PEX19 docking factor in the import of class I peroxisomal membrane proteins. *J. Cell Biol.* 164:863–875. http://dx.doi.org/10.1083/jcb.200311131

Fujiki, Y., A.L. Hubbard, S. Fowler, and P.B. Lazarow. 1982. Isolation of intracellular membranes by means of sodium carbonate treatment: application

to endoplasmic reticulum. *J. Cell Biol.* 93:97–102. http://dx.doi.org/10.1083/jcb.93.1.97

Fujiki, Y., Y. Matsuzono, T. Matsuzaki, and M. Fransen. 2006. Import of peroxisomal membrane proteins: the interplay of Pex3p- and Pex19p-mediated interactions. *Biochim. Biophys. Acta*. 1763:1639–1646. http://dx.doi.org/10.1016/j.bbamcr.2006.09.030

Gandre-Babbe, S., and A.M. van der Bliek. 2008. The novel tail-anchored membrane protein Mff controls mitochondrial and peroxisomal fission in mammalian cells. *Mol. Biol. Cell*. 19:2402–2412. http://dx.doi.org/10.1091/mbc.E07-12-1287

Ghaedi, K., S. Tamura, K. Okumoto, Y. Matsuzono, and Y. Fujiki. 2000. The peroxin pex3p initiates membrane assembly in peroxisome biogenesis. *Mol. Biol. Cell*. 11:2085–2102.

Götte, K., W. Girzalsky, M. Linkert, E. Baumgart, S. Kammerer, W.-H. Kunau, and R. Erdmann. 1998. Pex19p, a farnesylated protein essential for peroxisome biogenesis. *Mol. Cell. Biol.* 18:616–628.

Halbach, A., S. Lorenzen, C. Landgraf, R. Volkmer-Engert, R. Erdmann, and H. Rottensteiner. 2005. Function of the PEX19-binding site of human adrenoleukodystrophy protein as targeting motif in man and yeast. PMP targeting is evolutionarily conserved. *J. Biol. Chem.* 280:21176–21182. http://dx.doi.org/10.1074/jbc.M501750200

Halbach, A., C. Landgraf, S. Lorenzen, K. Rosenkranz, R. Volkmer-Engert, R. Erdmann, and H. Rottensteiner. 2006. Targeting of the tail-anchored peroxisomal membrane proteins PEX26 and PEX15 occurs through C-terminal PEX19-binding sites. *J. Cell Sci.* 119:2508–2517. http://dx.doi.org/10.1242/jcs.02979

Hegde, R.S., and R.J. Keenan. 2011. Tail-anchored membrane protein insertion into the endoplasmic reticulum. *Nat. Rev. Mol. Cell Biol.* 12:787–798. http://dx.doi.org/10.1038/nrm3226

Hessa, T., A. Sharma, M. Mariappan, H.D. Eshleman, E. Gutierrez, and R.S. Hegde. 2011. Protein targeting and degradation are coupled for elimination of mislocalized proteins. *Nature*. 475:394–397. http://dx.doi.org/10.1038/nature10181

Ho, S.N., H.D. Hunt, R.M. Horton, J.K. Pullen, and L.R. Pease. 1989. Site-directed mutagenesis by overlap extension using the polymerase chain reaction. *Gene*. 77:51–59. http://dx.doi.org/10.1016/0378-1119(89)90358-2

Hoepfner, D., D. Schildknegt, I. Braakman, P. Philippsen, and H.F. Tabak. 2005. Contribution of the endoplasmic reticulum to peroxisome formation. *Cell*. 122:85–95. http://dx.doi.org/10.1016/j.cell.2005.04.025

Horie, C., H. Suzuki, M. Sakaguchi, and K. Mihara. 2002. Characterization of signal that directs C-tail-anchored proteins to mammalian mitochondrial outer membrane. *Mol. Biol. Cell*. 13:1615–1625. http://dx.doi.org/10.1091/mbc.01-12-0570

Horton, R.M., H.D. Hunt, S.N. Ho, J.K. Pullen, and L.R. Pease. 1989. Engineering hybrid genes without the use of restriction enzymes: gene splicing by overlap extension. *Gene*. 77:61–68. http://dx.doi.org/10.1016/0378-1119(89)90359-4

Isenmann, S., Y. Khew-Goodall, J. Gamble, M. Vadas, and B.W. Wattenberg. 1998. A splice-isoform of vesicle-associated membrane protein-1 (VAMP-1) contains a mitochondrial targeting signal. *Mol. Biol. Cell*. 9:1649–1660.

Jones, J.M., J.C. Morrell, and S.J. Gould. 2004. PEX19 is a predominantly cytosolic chaperone and import receptor for class 1 peroxisomal membrane proteins. *J. Cell Biol.* 164:57–67. http://dx.doi.org/10.1083/jcb.200304111

Jonikas, M.C., S.R. Collins, V. Denic, E. Oh, E.M. Quan, V. Schmid, J. Weibezahn, B. Schwappach, P. Walter, J.S. Weissman, and M. Schuldiner. 2009. Comprehensive characterization of genes required for protein folding in the endoplasmic reticulum. *Science*. 323:1693–1697. http://dx.doi.org/10.1126/science.1167983

Kanaji, S., J. Iwahashi, Y. Kida, M. Sakaguchi, and K. Mihara. 2000. Characterization of the signal that directs Tom20 to the mitochondrial outer membrane. *J. Cell Biol.* 151:277–288. http://dx.doi.org/10.1083/jcb.151.2.277

Kaufmann, T., S. Schlipf, J. Sanz, K. Neubert, R. Stein, and C. Borner. 2003. Characterization of the signal that directs Bcl-x_L, but not Bcl-2, to the mitochondrial outer membrane. *J. Cell Biol.* 160:53–64. http://dx.doi.org/10.1083/jcb.200210084

Kemper, C., S.J. Habib, G. Engl, P. Heckmeyer, K.S. Dimmer, and D. Rapaport. 2008. Integration of tail-anchored proteins into the mitochondrial outer membrane does not require any known import components. *J. Cell Sci.* 121:1990–1998. http://dx.doi.org/10.1242/jcs.024034

Kim, P.K., R.T. Mullen, U. Schumann, and J. Lippincott-Schwartz. 2006. The origin and maintenance of mammalian peroxisomes involves a de novo PEX16-dependent pathway from the ER. *J. Cell Biol.* 173:521–532. http://dx.doi.org/10.1083/jcb.200601036

Kinoshita, N., K. Ghaedi, N. Shimozawa, R.J.A. Wanders, Y. Matsuzono, T. Imanaka, K. Okumoto, Y. Suzuki, N. Kondo, and Y. Fujiki. 1998. Newly identified Chinese hamster ovary cell mutants are defective in biogenesis of peroxisomal membrane vesicles (Peroxisomal ghosts), representing a novel complementation group in mammals. *J. Biol. Chem.* 273:24122–24130. http://dx.doi.org/10.1074/jbc.273.37.24122

Kobayashi, S., A. Tanaka, and Y. Fujiki. 2007. Fis1, DLP1, and Pex11p coordinately regulate peroxisome morphogenesis. *Exp. Cell Res.* 313:1675–1686. http://dx.doi.org/10.1016/j.yexcr.2007.02.028

Koch, A., Y. Yoon, N.A. Bonekamp, M.A. McNiven, and M. Schrader. 2005. A role for Fis1 in both mitochondrial and peroxisomal fission in mammalian cells. *Mol. Biol. Cell*. 16:5077–5086. http://dx.doi.org/10.1091/mbc.E05-02-0159

Kuroda, R., T. Ikenoue, M. Honsho, S. Tsujimoto, J.Y. Mitoma, and A. Ito. 1998. Charged amino acids at the carboxyl-terminal portions determine the intracellular locations of two isoforms of cytochrome b5. *J. Biol. Chem.* 273:31097–31102. http://dx.doi.org/10.1074/jbc.273.47.31097

Kutay, U., E. Hartmann, and T.A. Rapoport. 1993. A class of membrane proteins with a C-terminal anchor. *Trends Cell Biol.* 3:72–75. http://dx.doi.org/10.1016/0962-8924(93)90066-A

Kutay, U., G. Ahnert-Hilger, E. Hartmann, B. Wiedenmann, and T.A. Rapoport. 1995. Transport route for synaptobrevin via a novel pathway of insertion into the endoplasmic reticulum membrane. *EMBO J.* 14:217–223.

Lam, S.K., N. Yoda, and R. Schekman. 2010. A vesicle carrier that mediates peroxisome protein traffic from the endoplasmic reticulum. *Proc. Natl. Acad. Sci. USA*. 107:21523–21528. http://dx.doi.org/10.1073/pnas.1013397107

Leznicki, P., A. Clancy, B. Schwappach, and S. High. 2010. Bat3 promotes the membrane integration of tail-anchored proteins. *J. Cell Sci.* 123:2170–2178. http://dx.doi.org/10.1242/jcs.066738

Ma, C., G. Agrawal, and S. Subramani. 2011. Peroxisome assembly: matrix and membrane protein biogenesis. *J. Cell Biol.* 193:7–16. http://dx.doi.org/10.1083/jcb.201010022

Mariappan, M., X. Li, S. Stefanovic, A. Sharma, A. Mateja, R.J. Keenan, and R.S. Hegde. 2010. A ribosome-associating factor chaperones tail-anchored membrane proteins. *Nature*. 466:1120–1124. http://dx.doi.org/10.1038/nature09296

Matsumoto, N., S. Tamura, and Y. Fujiki. 2003. The pathogenic peroxin Pex26p recruits the Pex1p-Pex6p AAA ATPase complexes to peroxisomes. *Nat. Cell Biol.* 5:454–460. http://dx.doi.org/10.1038/ncb982

Matsuzaki, T., and Y. Fujiki. 2008. The peroxisomal membrane protein import receptor Pex3p is directly transported to peroxisomes by a novel Pex19p- and Pex16p-dependent pathway. *J. Cell Biol.* 183:1275–1286. http://dx.doi.org/10.1083/jcb.200806062

Matsuzono, Y., and Y. Fujiki. 2006. *In vitro* transport of membrane proteins to peroxisomes by shuttling receptor Pex19p. *J. Biol. Chem.* 281:36–42. http://dx.doi.org/10.1074/jbc.M509819200

Matsuzono, Y., N. Kinoshita, S. Tamura, N. Shimozawa, M. Hamasaki, K. Ghaedi, R.J.A. Wanders, Y. Suzuki, N. Kondo, and Y. Fujiki. 1999. Human *PEX19*: cDNA cloning by functional complementation, mutation analysis in a patient with Zellweger syndrome, and potential role in peroxisomal membrane assembly. *Proc. Natl. Acad. Sci. USA*. 96:2116–2121. http://dx.doi.org/10.1073/pnas.96.5.2116

Matsuzono, Y., T. Matsuzaki, and Y. Fujiki. 2006. Functional domain mapping of peroxin Pex19p: interaction with Pex3p is essential for function and translocation. *J. Cell Sci.* 119:3539–3550. http://dx.doi.org/10.1242/jcs.03100

Mukai, S., and Y. Fujiki. 2006. Molecular mechanisms of import of peroxisome-targeting signal type 2 (PTS2) proteins by PTS2 receptor Pex7p and PTS1 receptor Pex5pL. *J. Biol. Chem.* 281:37311–37320. http://dx.doi.org/10.1074/jbc.M607178200

Mukai, S., K. Ghaedi, and Y. Fujiki. 2002. Intracellular localization, function, and dysfunction of the peroxisome-targeting signal type 2 receptor, Pex7p, in mammalian cells. *J. Biol. Chem.* 277:9548–9561. http://dx.doi.org/10.1074/jbc.M108635200

Mullen, R.T., C.S. Lisenbee, J.A. Miernyk, and R.N. Trelease. 1999. Peroxisomal membrane ascorbate peroxidase is sorted to a membranous network that resembles a subdomain of the endoplasmic reticulum. *Plant Cell*. 11:2167–2185.

Nemoto, Y., and P. De Camilli. 1999. Recruitment of an alternatively spliced form of synaptojanin 2 to mitochondria by the interaction with the PDZ domain of a mitochondrial outer membrane protein. *EMBO J.* 18:2991–3006. http://dx.doi.org/10.1093/emboj/18.11.2991

Nuttall, J.M., A. Motley, and E.H. Hettema. 2011. Peroxisome biogenesis: recent advances. *Curr. Opin. Cell Biol.* 23:421–426. http://dx.doi.org/10.1016/j.ceb.2011.05.005

Otera, H., K. Okumoto, K. Tateishi, Y. Ikoma, E. Matsuda, M. Nishimura, T. Tsukamoto, T. Osumi, K. Ohashi, O. Higuchi, and Y. Fujiki. 1998. Peroxisome targeting signal type 1 (PTS1) receptor is involved in import of both PTS1 and PTS2: studies with *PEX5*-defective CHO cell mutants. *Mol. Cell. Biol.* 18:388–399.

Otera, H., T. Harano, M. Honsho, K. Ghaedi, S. Mukai, A. Tanaka, A. Kawai, N. Shimizu, and Y. Fujiki. 2000. The mammalian peroxin Pex5pL, the longer isoform of the mobile peroxisome targeting signal (PTS) type 1 transporter, translocates the Pex7p.PTS2 protein complex into peroxisomes via its initial docking site, Pex14p. *J. Biol. Chem.* 275:21703–21714. http://dx.doi.org/10.1074/jbc.M000720200

Pinto, M.P., C.P. Grou, I.S. Alencastre, M.E. Oliveira, C. Sá-Miranda, M. Fransen, and J.E. Azevedo. 2006. The import competence of a peroxisomal membrane protein is determined by Pex19p before the docking step. *J. Biol. Chem.* 281:34492–34502. http://dx.doi.org/10.1074/jbc.M607183200

Rabu, C., P. Wipf, J.L. Brodsky, and S. High. 2008. A precursor-specific role for Hsp40/Hsc70 during tail-anchored protein integration at the endoplasmic reticulum. *J. Biol. Chem.* 283:27504–27513. http://dx.doi.org/10.1074/jbc.M804591200

Rottensteiner, H., A. Kramer, S. Lorenzen, K. Stein, C. Landgraf, R. Volkmer-Engert, and R. Erdmann. 2004. Peroxisomal membrane proteins contain common Pex19p-binding sites that are an integral part of their targeting signals. *Mol. Biol. Cell*. 15:3406–3417. http://dx.doi.org/10.1091/mbc.E04-03-0188

Rucktäschel, R., W. Girzalsky, and R. Erdmann. 2011. Protein import machineries of peroxisomes. *Biochim. Biophys. Acta*. 1808:892–900. http://dx.doi.org/10.1016/j.bbamem.2010.07.020

Sacksteder, K.A., J.M. Jones, S.T. South, X. Li, Y. Liu, and S.J. Gould. 2000. PEX19 binds multiple peroxisomal membrane proteins, is predominantly cytoplasmic, and is required for peroxisome membrane synthesis. *J. Cell Biol.* 148:931–944. http://dx.doi.org/10.1083/jcb.148.5.931

Sato, Y., H. Shibata, H. Nakano, Y. Matsuzono, Y. Kashiwayama, Y. Kobayashi, Y. Fujiki, T. Imanaka, and H. Kato. 2008. Characterization of the interaction between recombinant human peroxin Pex3p and Pex19p: identification of TRP-104 IN Pex3p as a critical residue for the interaction. *J. Biol. Chem.* 283:6136–6144. http://dx.doi.org/10.1074/jbc.M706139200

Sato, Y., H. Shibata, T. Nakatsu, H. Nakano, Y. Kashiwayama, T. Imanaka, and H. Kato. 2010. Structural basis for docking of peroxisomal membrane protein carrier Pex19p onto its receptor Pex3p. *EMBO J.* 29:4083–4093. http://dx.doi.org/10.1038/emboj.2010.293

Schuldiner, M., J. Metz, V. Schmid, V. Denic, M. Rakwalska, H.D. Schmitt, B. Schwappach, and J.S. Weissman. 2008. The GET complex mediates insertion of tail-anchored proteins into the ER membrane. *Cell*. 134:634–645. http://dx.doi.org/10.1016/j.cell.2008.06.025

Setoguchi, K., H. Otera, and K. Mihara. 2006. Cytosolic factor- and TOM-independent import of C-tail-anchored mitochondrial outer membrane proteins. *EMBO J.* 25:5635–5647. http://dx.doi.org/10.1038/sj.emboj.7601438

Shibata, H., Y. Kashiwayama, T. Imanaka, and H. Kato. 2004. Domain architecture and activity of human Pex19p, a chaperone-like protein for intracellular trafficking of peroxisomal membrane proteins. *J. Biol. Chem.* 279:38486–38494. http://dx.doi.org/10.1074/jbc.M402204200

Shimizu, N., R. Itoh, Y. Hirono, H. Otera, K. Ghaedi, K. Tateishi, S. Tamura, K. Okumoto, T. Harano, S. Mukai, and Y. Fujiki. 1999. The peroxin Pex14p. cDNA cloning by functional complementation on a Chinese hamster ovary cell mutant, characterization, and functional analysis. *J. Biol. Chem.* 274:12593–12604. http://dx.doi.org/10.1074/jbc.274.18.12593

Shimozawa, N., T. Tsukamoto, Y. Suzuki, T. Orii, and Y. Fujiki. 1992. Animal cell mutants represent two complementation groups of peroxisome-defective Zellweger syndrome. *J. Clin. Invest.* 90:1864–1870. http://dx.doi.org/10.1172/JCI116063

Snyder, W.B., K.N. Faber, T.J. Wenzel, A. Koller, G.H. Lüers, L. Rangell, G.A. Keller, and S. Subramani. 1999. Pex19p interacts with Pex3p and Pex10p and is essential for peroxisome biogenesis in *Pichia pastoris*. *Mol. Biol. Cell*. 10:1745–1761.

Soukupova, M., C. Sprenger, K. Gorgas, W.-H. Kunau, and G. Dodt. 1999. Identification and characterization of the human peroxin PEX3. *Eur. J. Cell Biol.* 78:357–374. http://dx.doi.org/10.1016/S0171-9335(99)80078-8

Stefanovic, S., and R.S. Hegde. 2007. Identification of a targeting factor for posttranslational membrane protein insertion into the ER. *Cell*. 128:1147–1159. http://dx.doi.org/10.1016/j.cell.2007.01.036

Tsukamoto, T., S. Yokota, and Y. Fujiki. 1990. Isolation and characterization of Chinese hamster ovary cell mutants defective in assembly of peroxisomes. *J. Cell Biol.* 110:651–660. http://dx.doi.org/10.1083/jcb.110.3.651

Van Ael, E., and M. Fransen. 2006. Targeting signals in peroxisomal membrane proteins. *Biochim. Biophys. Acta*. 1763:1629–1638. http://dx.doi.org/10.1016/j.bbamcr.2006.08.020

van der Zand, A., I. Braakman, and H.F. Tabak. 2010. Peroxisomal membrane proteins insert into the endoplasmic reticulum. *Mol. Biol. Cell*. 21:2057–2065. http://dx.doi.org/10.1091/mbc.E10-02-0082